Aortic valve: anatomical assessment and key information for surgical and percutaneous procedures - quantification tools

Victoria Delgado, MD, PhD
Hospital University Germans Trias i Pujol
Badalona, Spain

Disclosures

- Speaker fees from Edwards Lifesciences, GE Healthcare, Philips, Novartis and Medtronic.
- Consulting fees from Edwards Lifesciences, MSD and Novo Nordisk

Understanding anatomy of aortic valve and aortic root

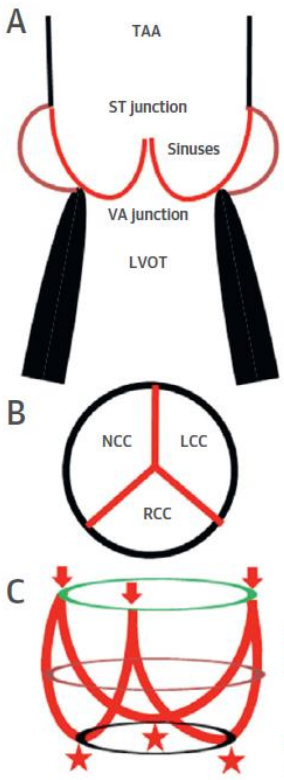

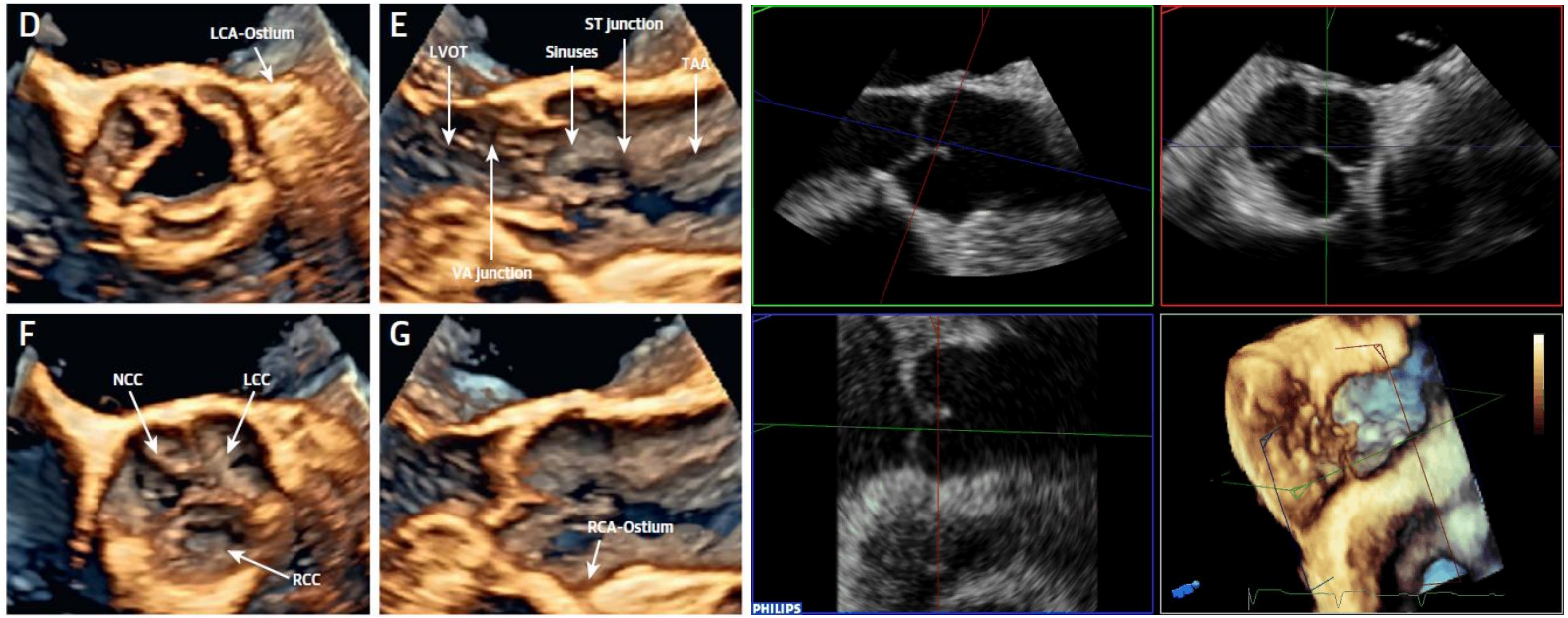

Sinotubular (ST-) junction
Crown-like ring of the insertion of the cups between the VA-and ST-junction
Nadirs of the cusps
Crown-like tips of the commissures between the cusps
Circle with the maximum diameter of the Sinus of Valsalva
Ventricular-aortic (VA-) junction = basal aortic annulus

Hagendorff et al J Am Coll Cardiol Img 2019;12:2225–44

Understanding anatomy of aortic valve and aortic root

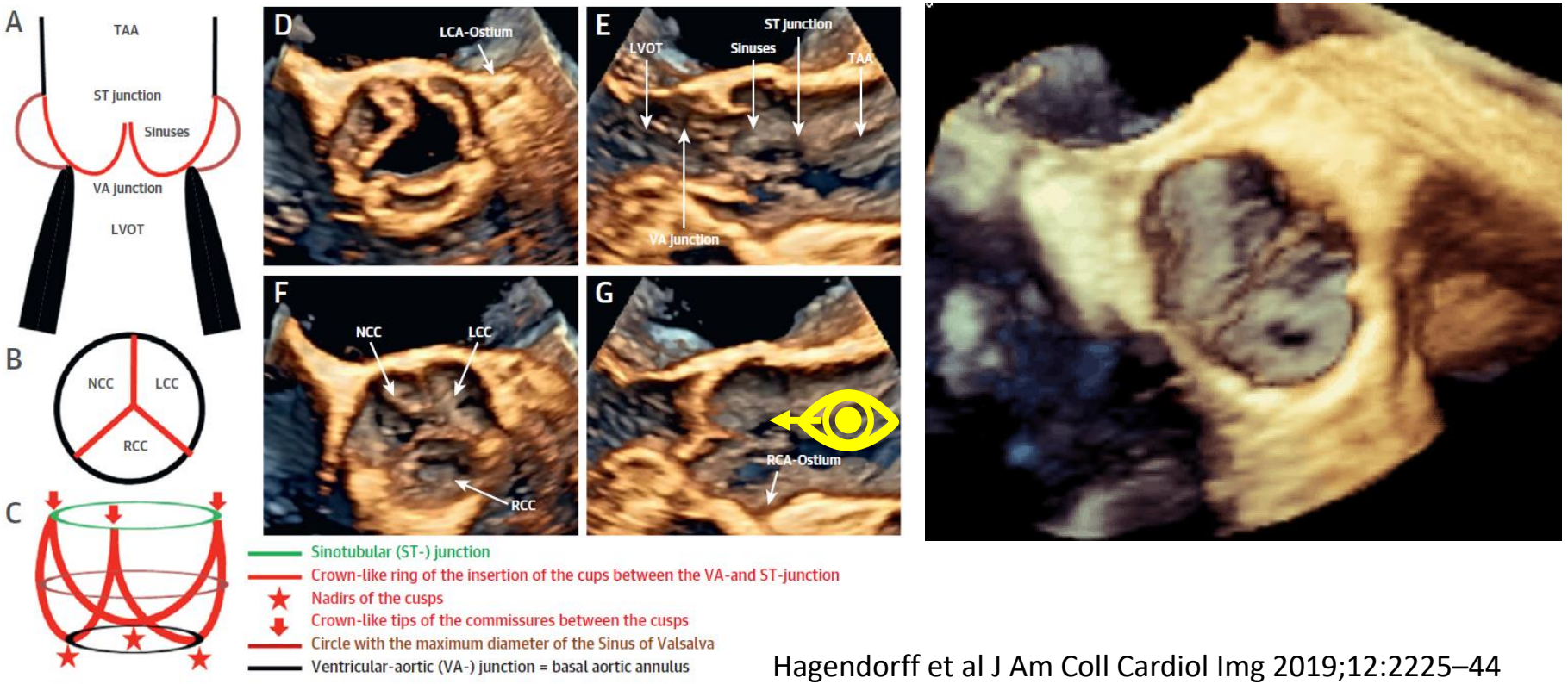

Hagendorff et al J Am Coll Cardiol Img 2019;12:2225–44

Understanding anatomy of aortic valve and aortic root

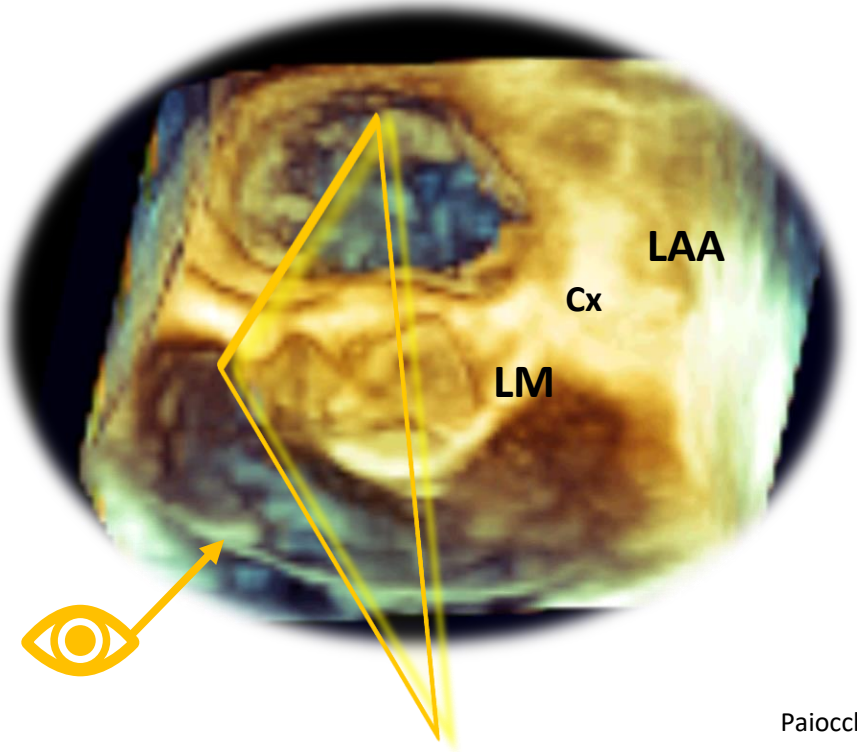

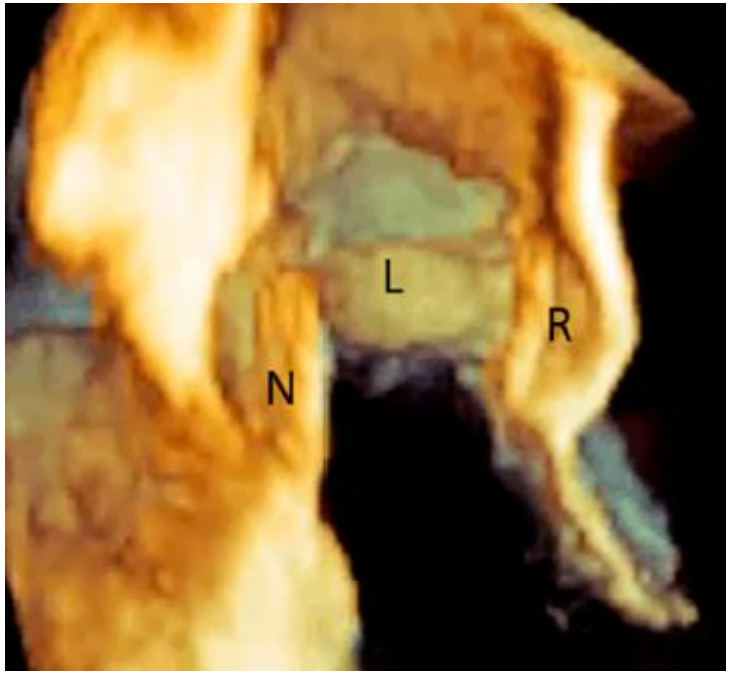

Paiocchi et al J. Cardiovasc. Dev. Dis. **2021**, 8, 51. https://doi.org/10.3390/jcdd8050051

Understanding anatomy of aortic valve and aortic root

tricuspid

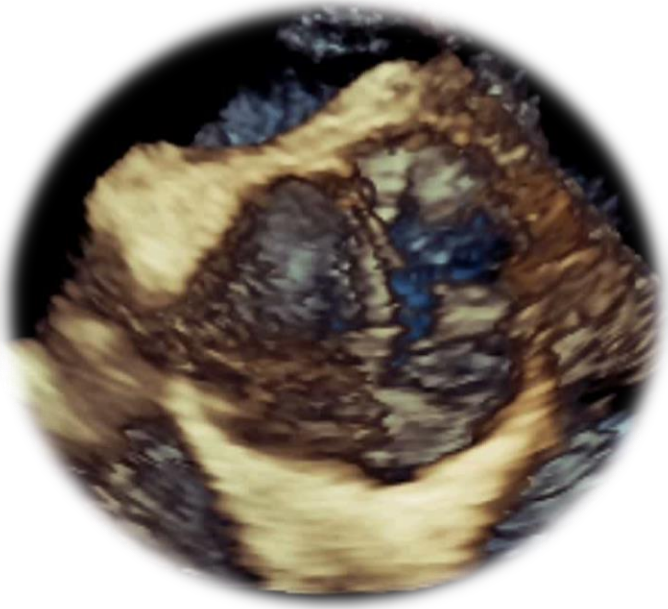

bicuspid

quadricuspid

Kendall et al CASE https://doi.org/10.1016/j.case.2022.11.006

Aortic valve pathology

Aortic stenosis
• Confirmation of severity of AS
• Anatomy and morphology of the aortic valve
• Coronary artery ostia height
• Selection of prosthesis size – annulus sizing
• Selection of procedural access

Aortic regurgitation
• Confirmation of severity of AR
• Anatomy and morphology of the aortic valve
• Mechanism of dysfunction

Aortic stenosis - severity

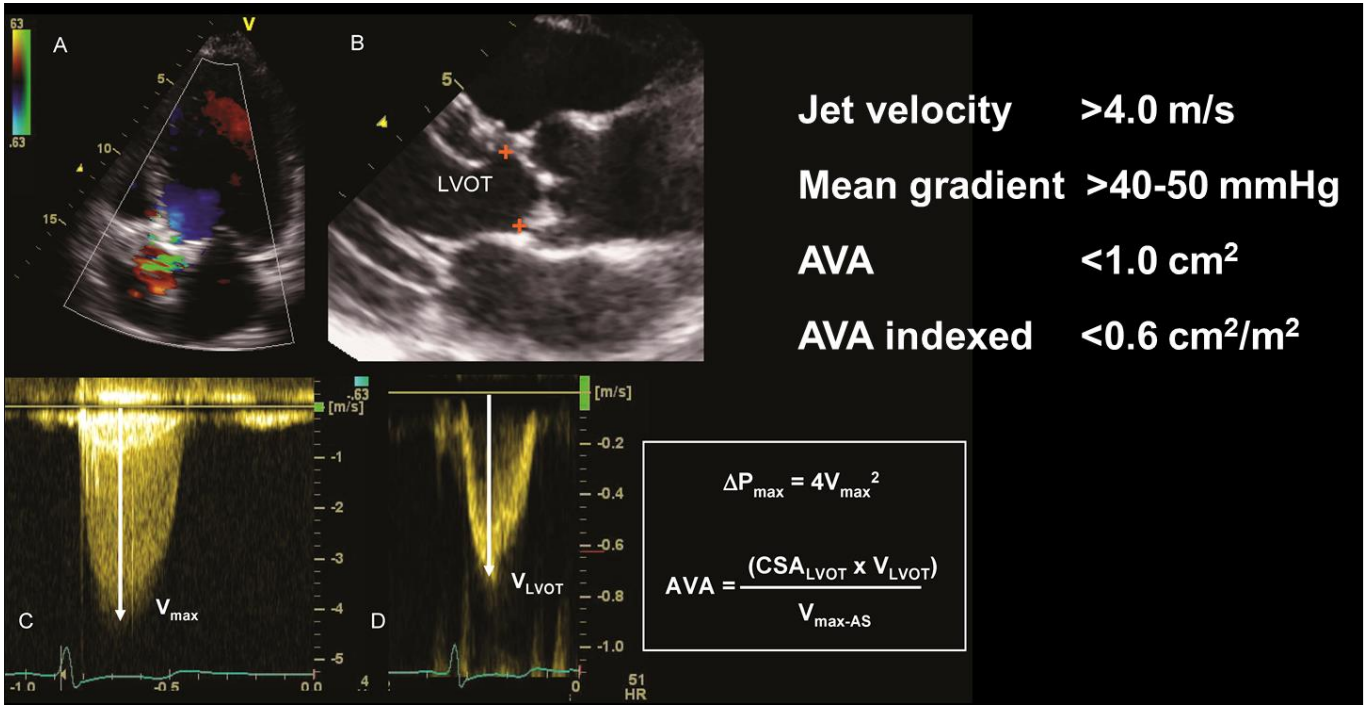

Baumgartner et al. EHJCVI 2017

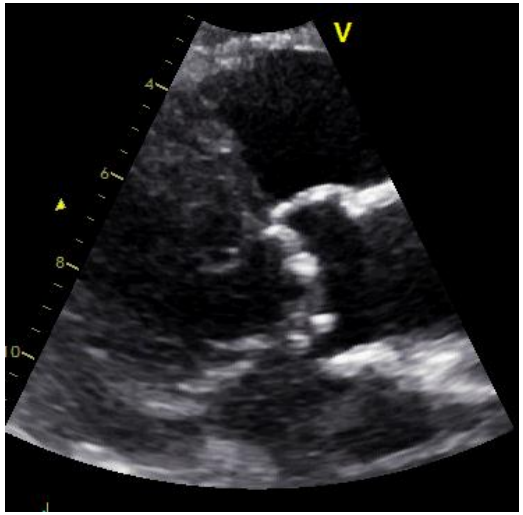

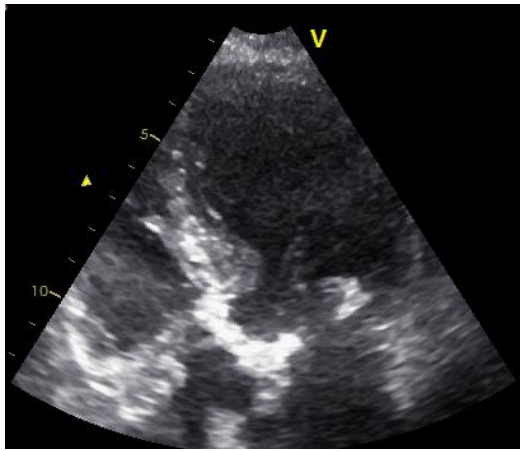

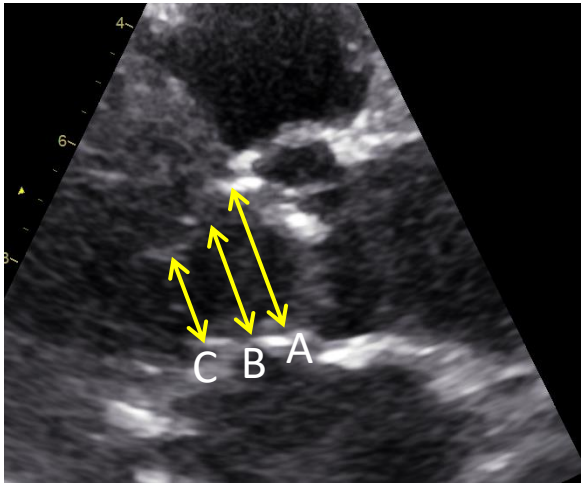

A: LVOT 20 mm; AVA 0.98 cm^2
B: LVOT 18 mm; AVA 0.75 cm^2
C: LVOT 15 mm; AVA 0.54 cm^2

Integration of 3D LVOT in continuity equation

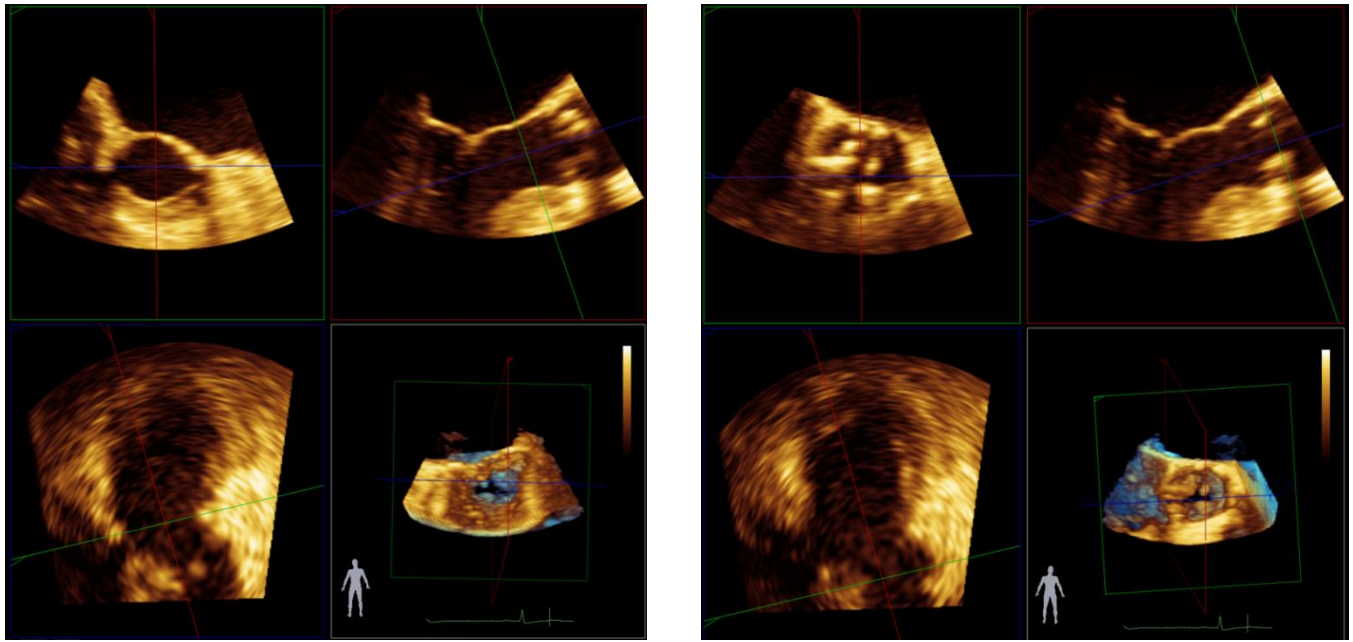

Variable	2D-TTE	2D-TEE	RT3D-TEE
Planimetry	1.01 (0.70–1.17)*	1.01 (0.83–1.10)*	0.96 (0.81–1.10)
Continuity equation	0.77 (0.64–0.94)	0.76 (0.62–1.0)	1.0 (0.79–1.2)†

Saitoh et al. Am J Cardiol 2012

Anatomical AVA from 3D

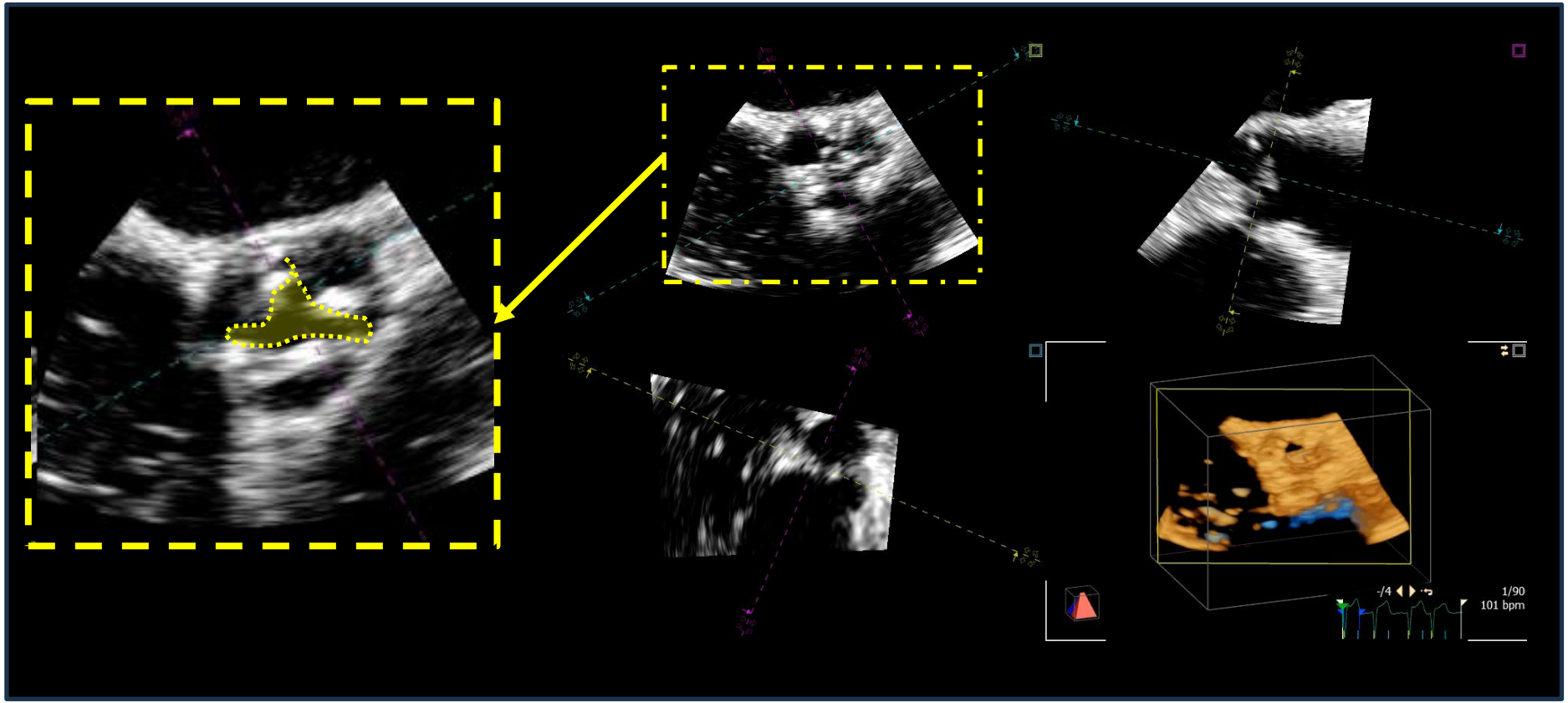

Coronary ostia height

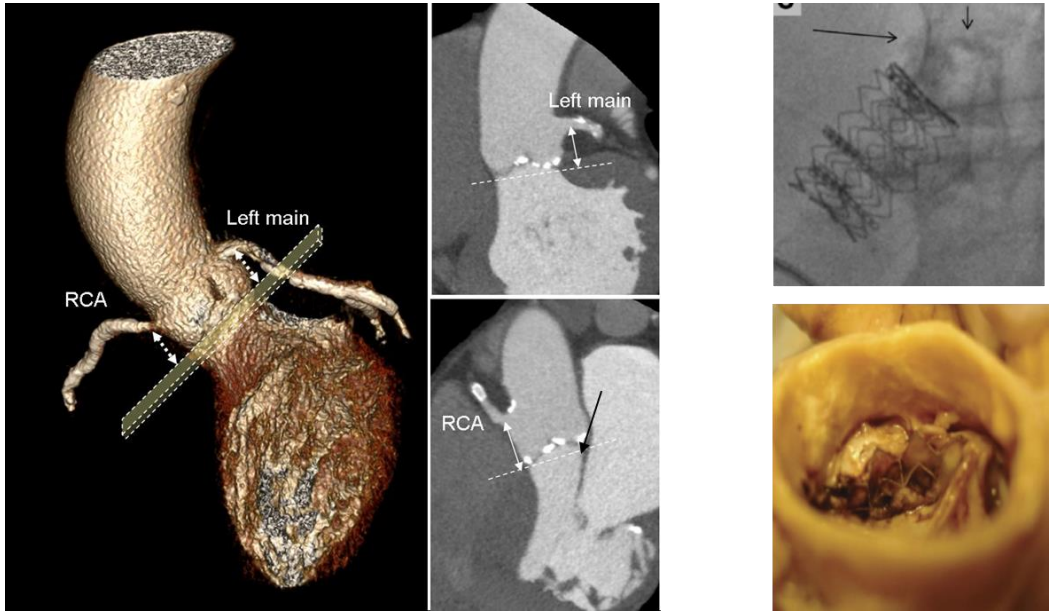

Occlusion of coronary ostia by bulky calcified leaflets uncommon but fatal

Masson et al. JACC Intervent 2009

Coronary ostia height

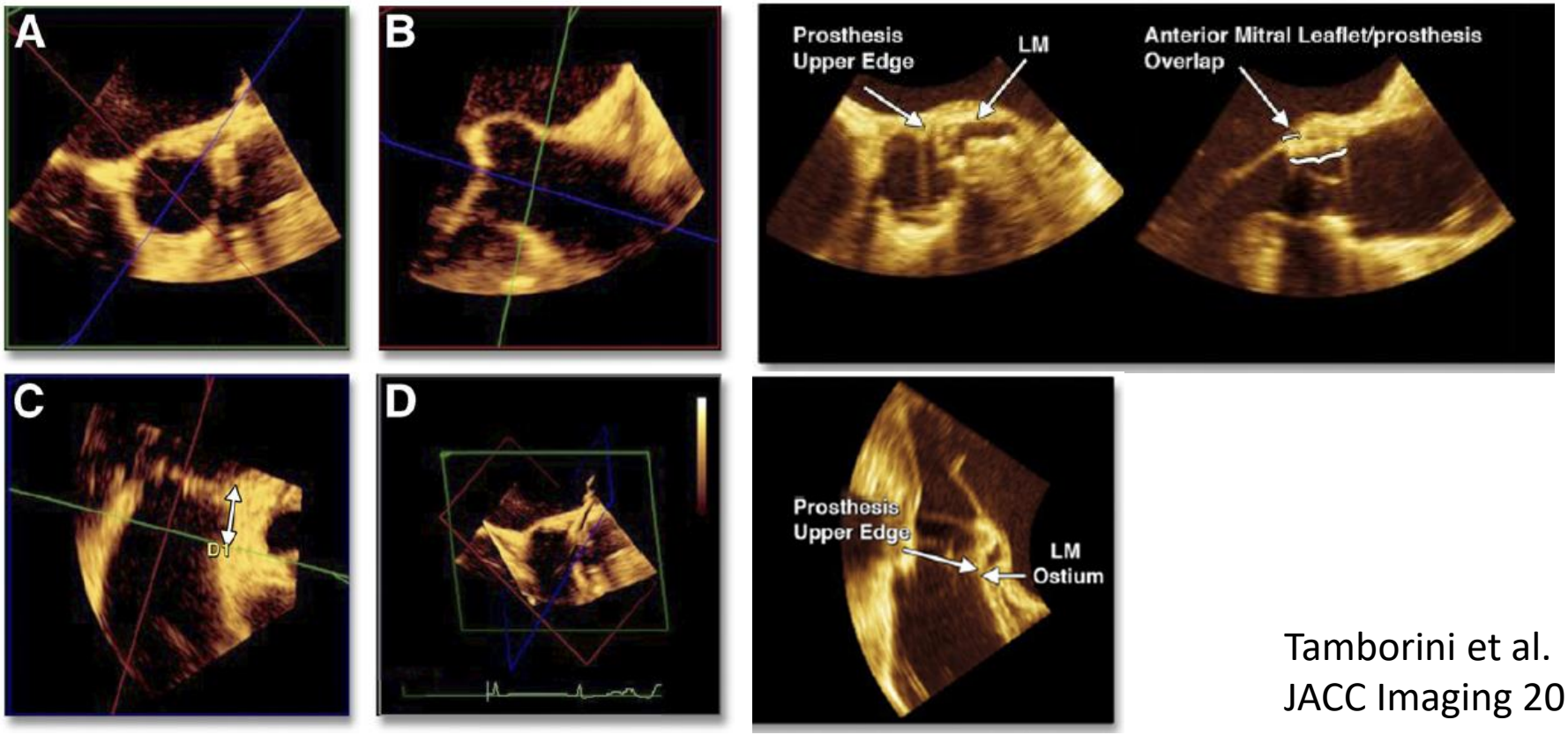

Tamborini et al.
JACC Imaging 2012

Prosthesis sizing

23 mm

26 mm

29 mm

Annulus Size by TEE

18 – 22 mm

21 – 25 mm

24 – 28 mm

Native Annulus Area	338 – 430 mm ^{2}	430 – 546 mm ^{2}	540 – 680 mm ^{2}
Area-derived Diameter	20.7 – 23.4 mm	23.4 – 26.4 mm	26.2 – 29.5 mm

Prosthesis sizing

Valve Size	23 mm	26 mm	29 mm	31 mm
				
Annulus Diameter	18-20 mm	20 - 23 mm	23 - 27 mm	26 - 29 mm
Annulus Perimeter	56.5 – 62.8 mm	62.8 - 72.3 mm	72.3 - 84.8 mm	81.6 - 91.1 mm
Annulus Area	254.5 - 314.2 mm^2	314.2 - 415.5 mm^2	415.5 - 572.6 mm^2	530.9 – 660.5 mm^2

Prosthesis sizing

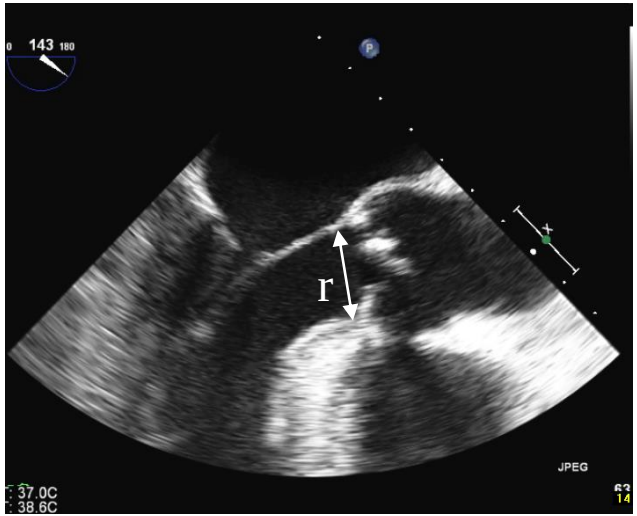

Circular area

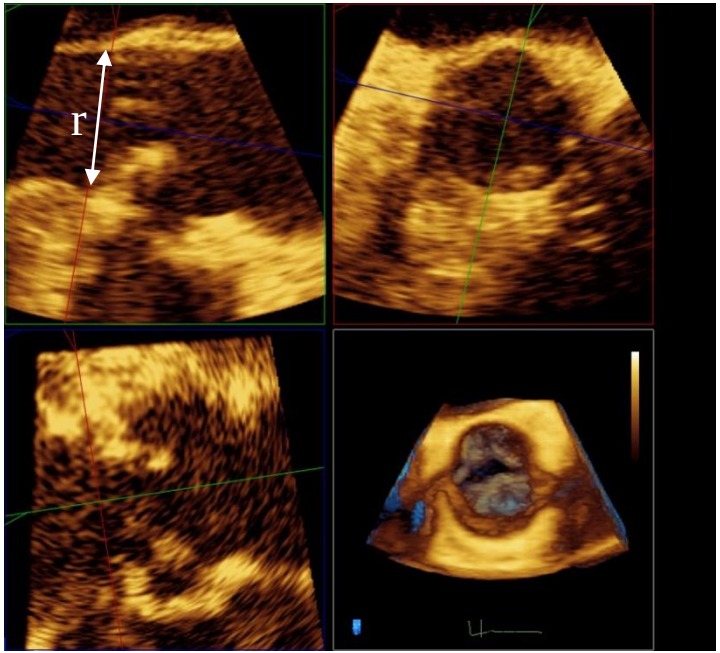

Circular area
Planimetered area

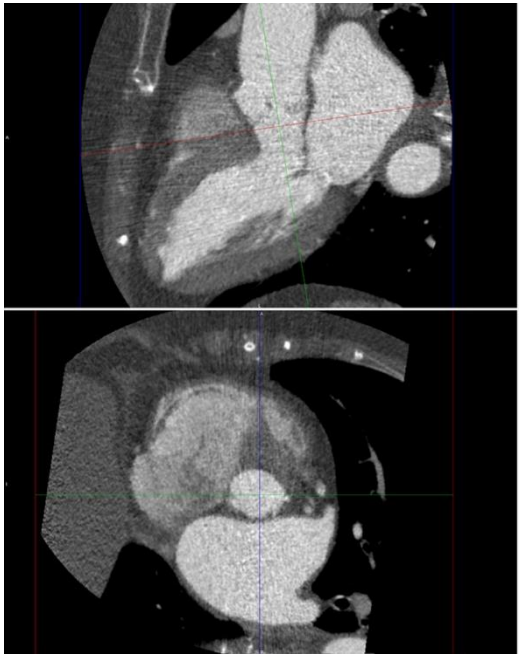

Planimetered area

Ng et al. Circulation Cardiovasc Imag 2010

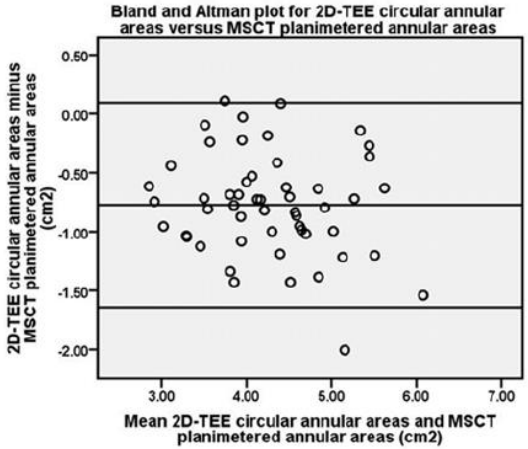

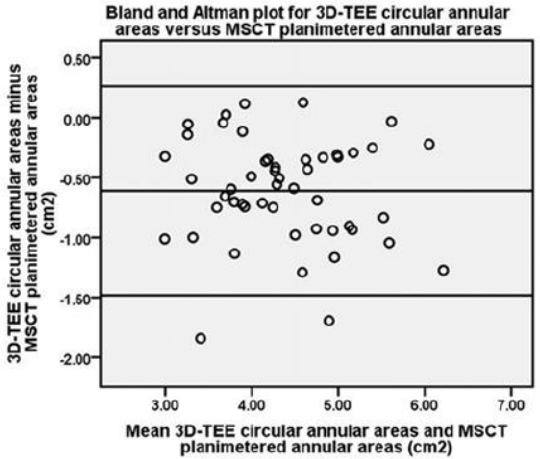

Compared to MSCT, 3D-TEE planimetered annular areas had the narrowest limits of agreement and least bias

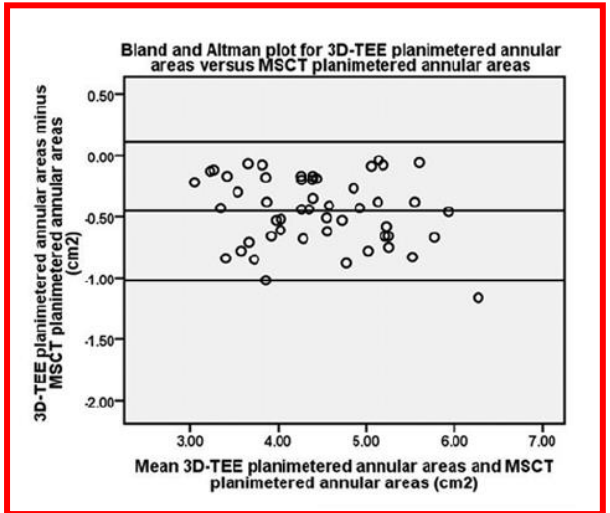

Ng et al. Circulation Cardiovasc Imag 2010

Automated algorithms

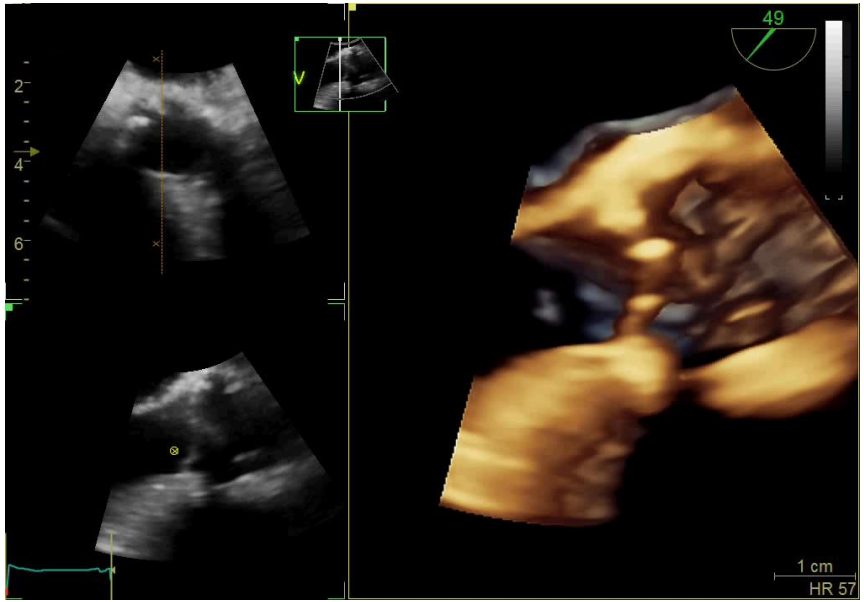

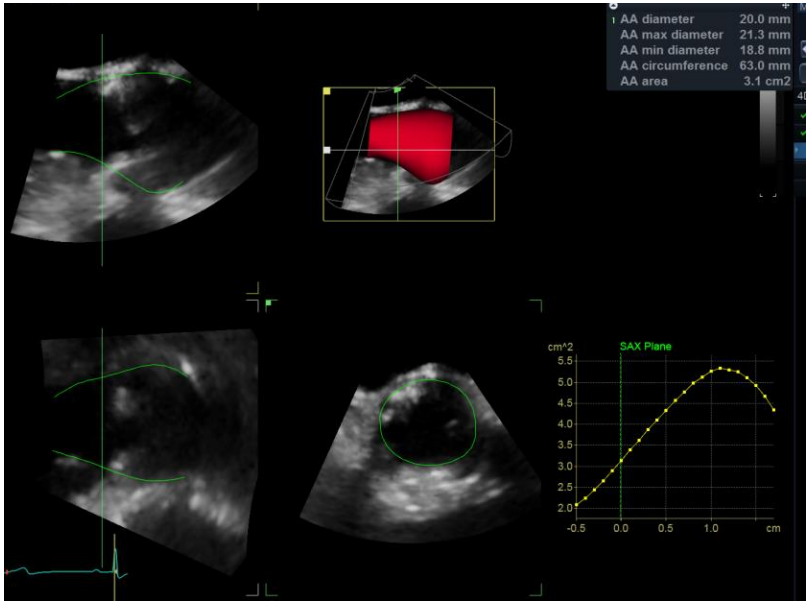

Automated algorithms

Area

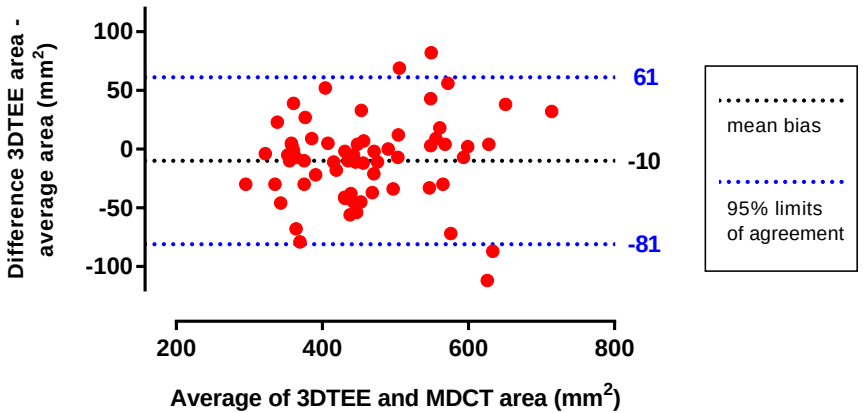

Perimeter

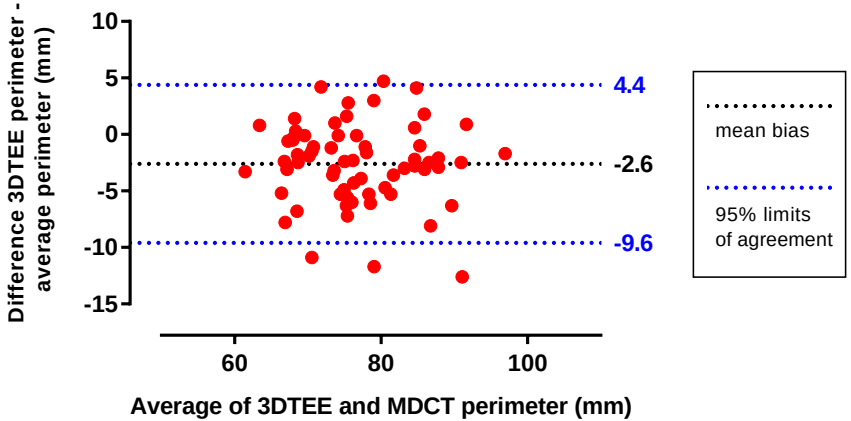

Podlesnikar et al. Am J Cardiol 2021

N = 65

Automated algorithms

Area measurement agreement according to AVC

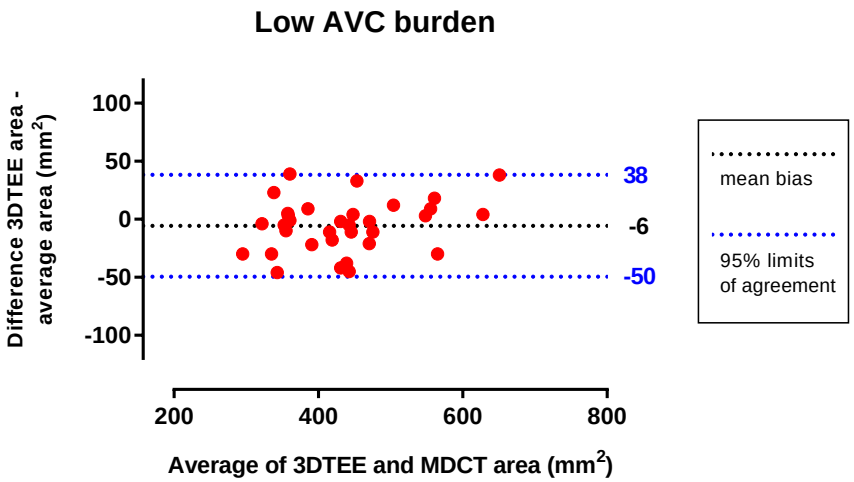

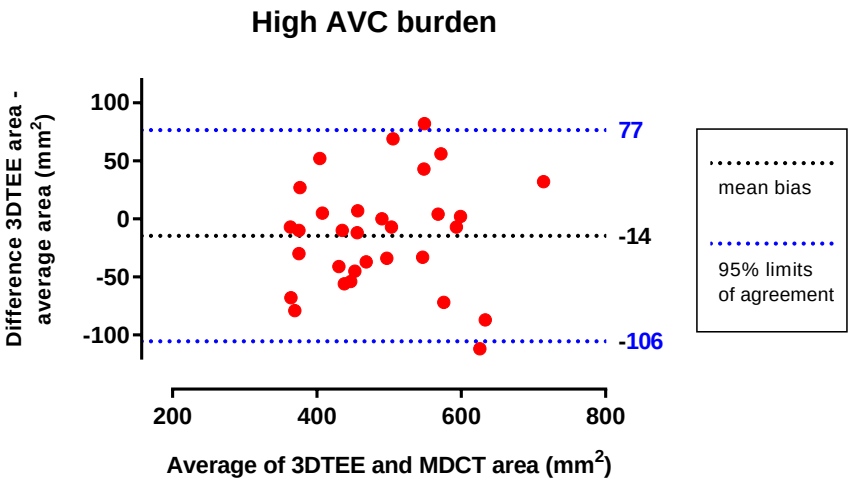

Podlesnikar et al. Am J Cardiol 2021

N = 65

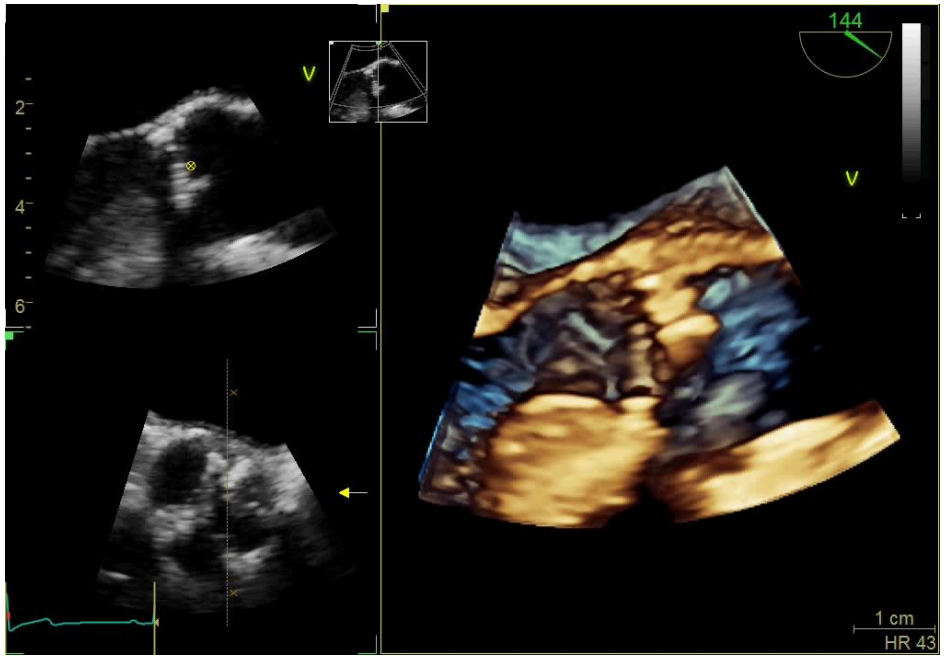
144
V
V
2
4
6
1 cm
HR 43

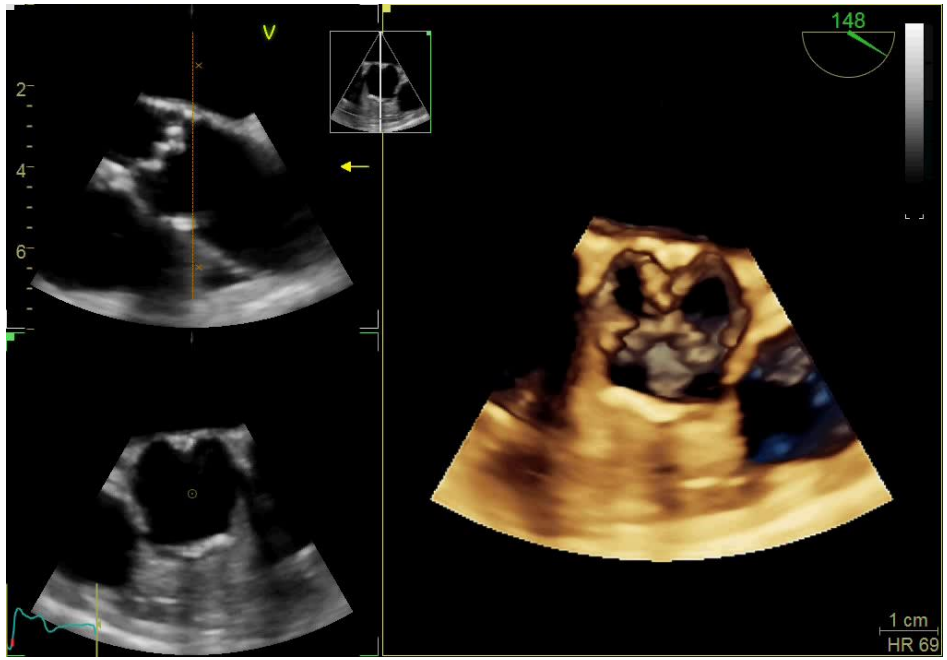
148
V
2
4
6
1 cm
HR 69

Procedural access

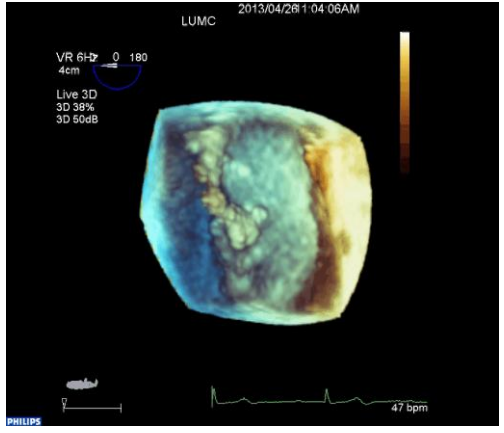

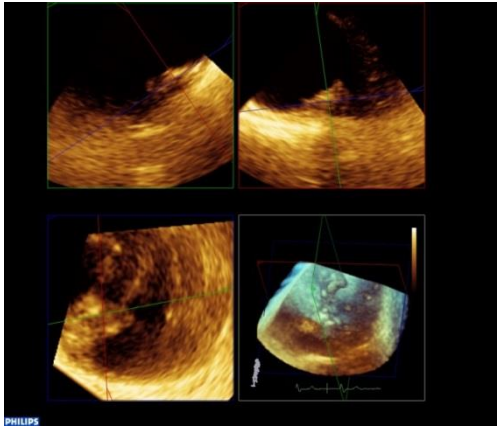

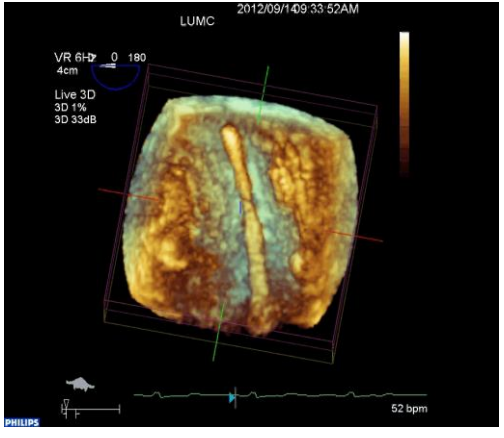

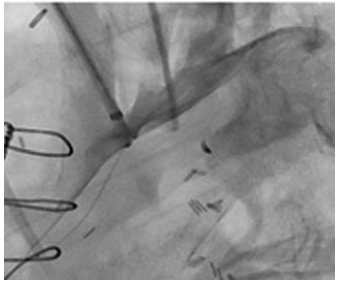

Protection devices

Nietlispach et al. JACC Intervent 2010

Procedural access

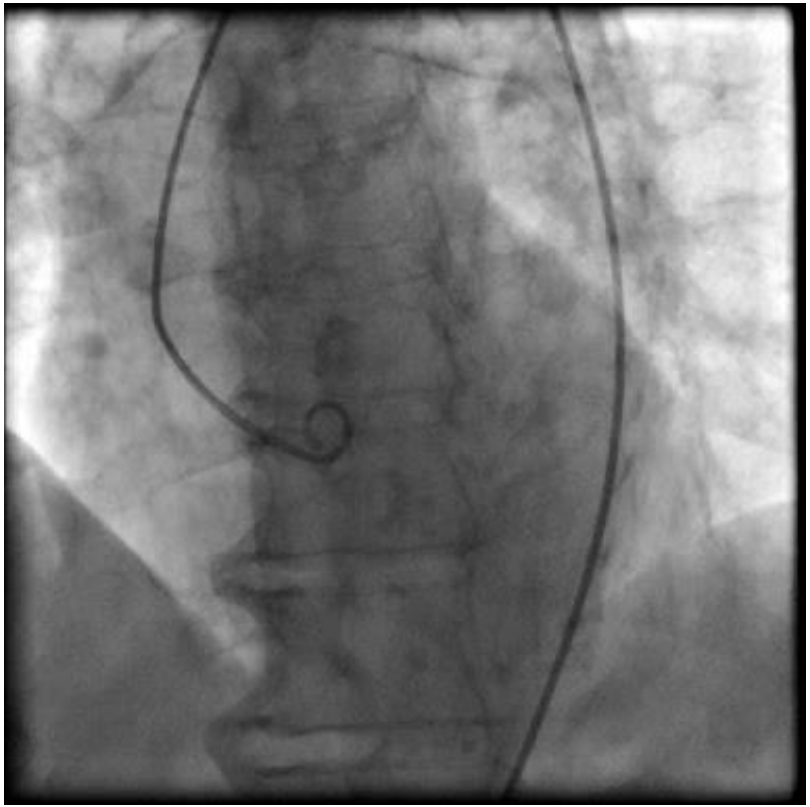

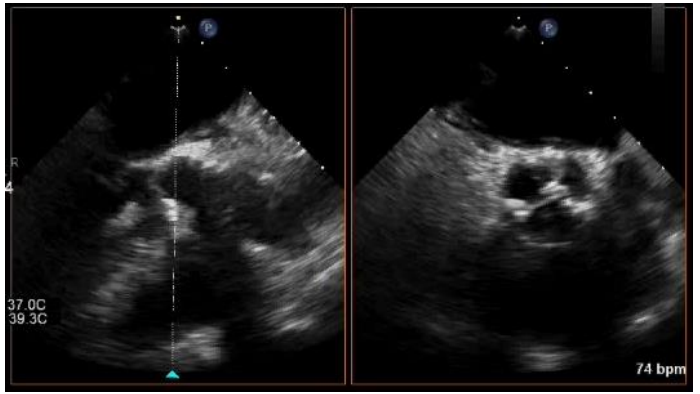

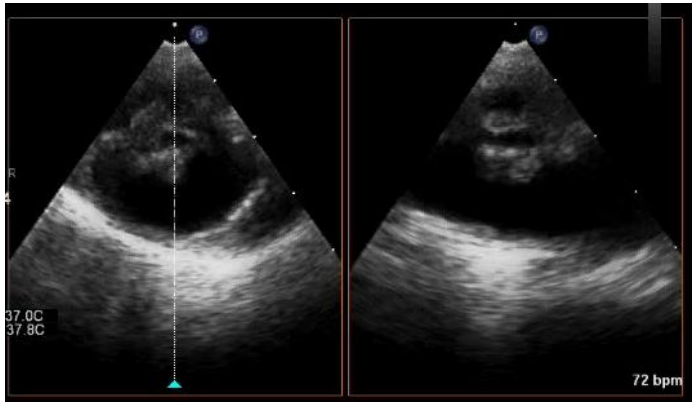

Aortic regurgitation

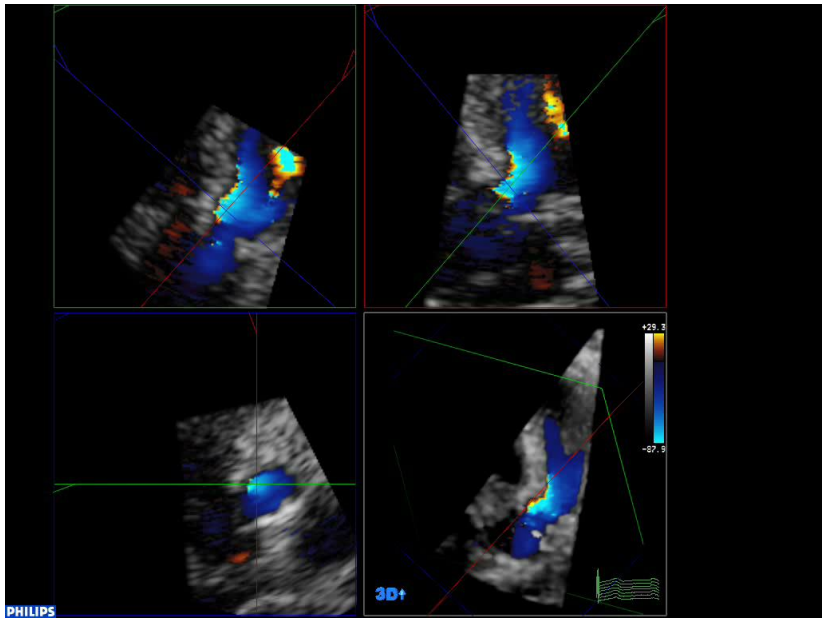

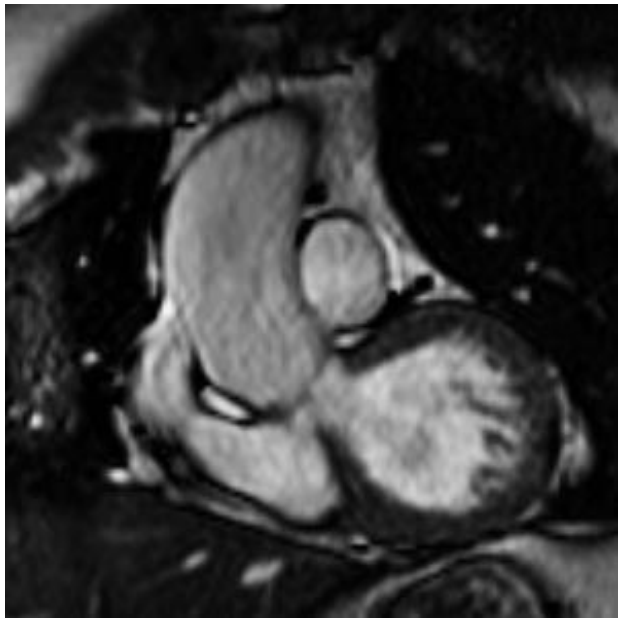

AR severity

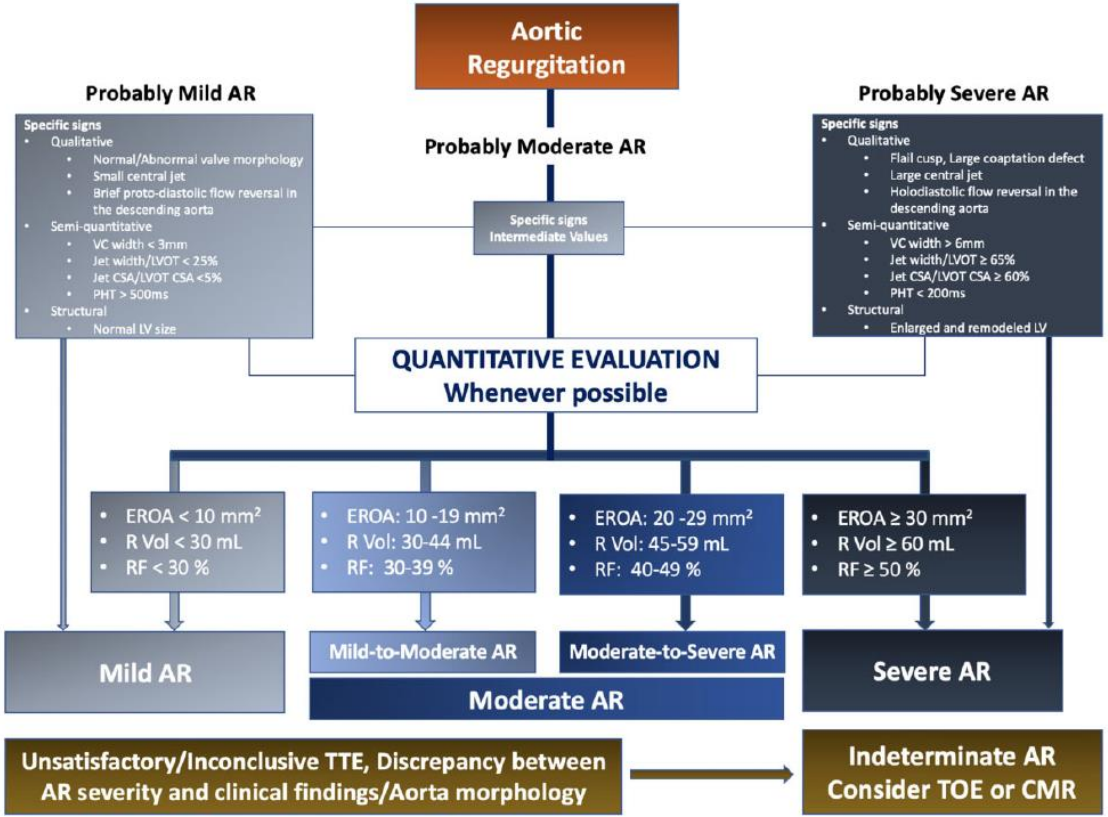

Table 7 Grading the severity of AR

AR severity classes[a]	Severe
AR severity sub-classes[a]	Severe (Grade 4 or 4+)
Qualitative parameters	
Aortic valve morphology	Abnormal/**flail/large coaptation defect**
Colour flow AR jet width[b]	**Large in central jet,** variable in eccentric jets
Color flow convergence	Large
CW signal of AR jet	Dense
Diastolic flow reversal in descending aorta[c]	**Holodiastolic flow reversal** (end-diastolic velocity ≥ 20 cm/s)
Diastolic flow reversal in abdominal aorta[c]	Present
Semi-quantitative parameters	
VC width (mm)	**>6**
Jet width/LVOT diameter (%)	**≥65**
Jet CSA/LVOT CSA (%)	**≥60**
Pressure half-time (ms)[c,d]	**<200**
Quantitative parameters	
EROA (mm^2)	≥30
R Vol (mL)	≥60
RF (%)	≥50
CMR parameters	
RF (%)	≥ 50
Structural parameters	
LV size[e]	Usually dilated

European Heart Journal - Cardiovascular Imaging (2022) 23, e171–e232

AR severity

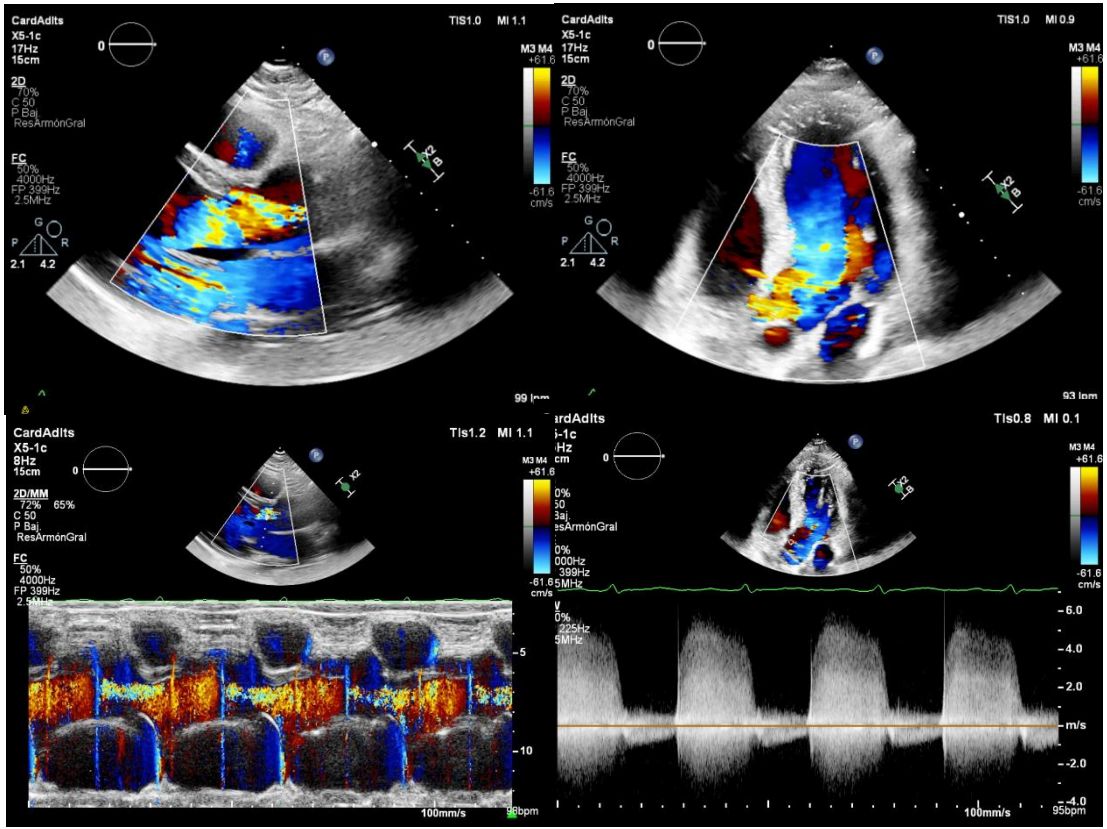

Table 7 Grading the severity of AR

AR severity classes[a]	**Severe**
AR severity sub-classes[a]	**Severe (Grade 4 or 4+)**
Qualitative parameters	
Aortic valve morphology	Abnormal/**flail/large coaptation defect**
Colour flow AR jet width[b]	**Large in central jet,** variable in eccentric jets
Color flow convergence	Large
CW signal of AR jet	Dense
Diastolic flow reversal in descending aorta[c]	**Holodiastolic flow reversal** (end-diastolic velocity ≥ 20 cm/s)
Diastolic flow reversal in abdominal aorta[c]	Present
Semi-quantitative parameters	
VC width (mm)	**>6**
Jet width/LVOT diameter (%)	**≥65**
Jet CSA/LVOT CSA (%)	**≥60**
Pressure half-time (ms)[c,d]	**<200**
Quantitative parameters	
EROA (mm^2)	≥30
R Vol (mL)	≥60
RF (%)	≥50
CMR parameters	
RF (%)	≥ 50
Structural parameters	
LV size[e]	Usually dilated

AR severity

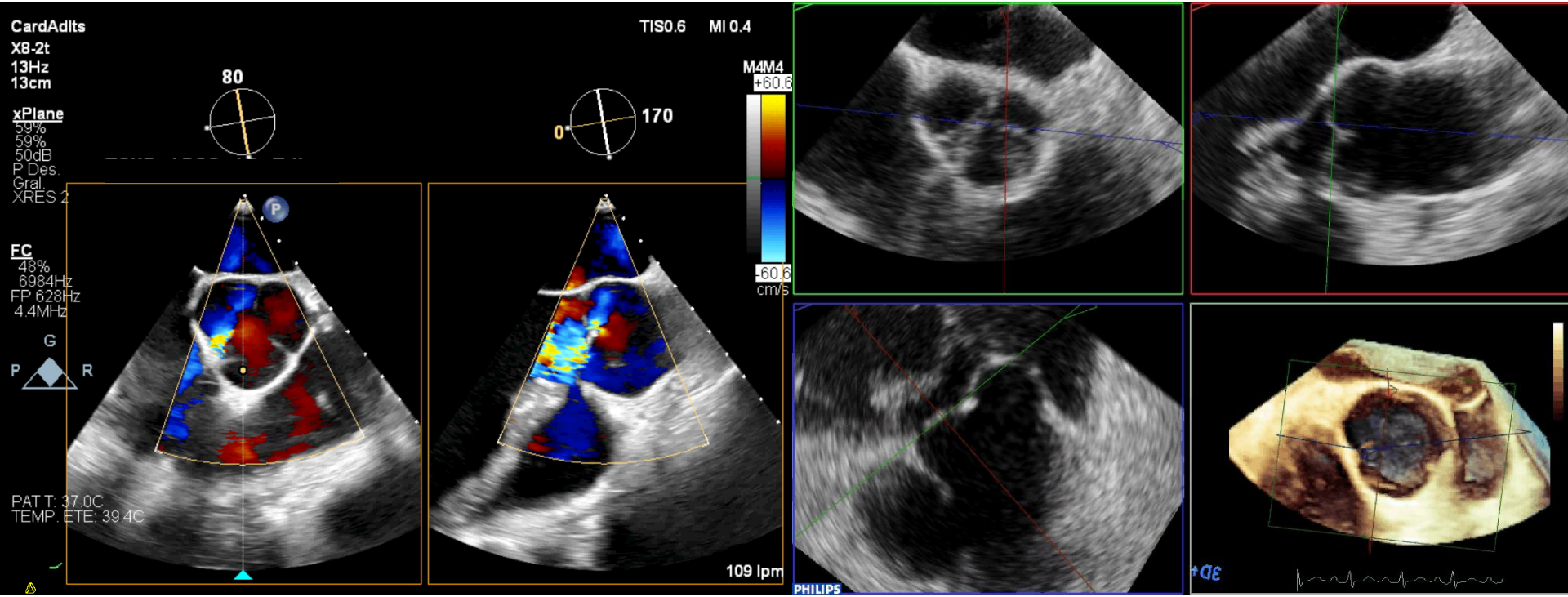
CardAdlts
X8-2t
13Hz
13cm
xPlane
59%
59%
50dB
P Des.
Gral.
XRES 2
FC
48%
6984Hz
FP 628Hz
4.4MHz
G
P
R
80
0
170
TIS0.6
MI 0.4
M4M4
+60.6
-60.6
cm/s
PAT T: 37.0C
TEMP: ETE: 39.4C
109 lpm
PHILIPS

AR severity

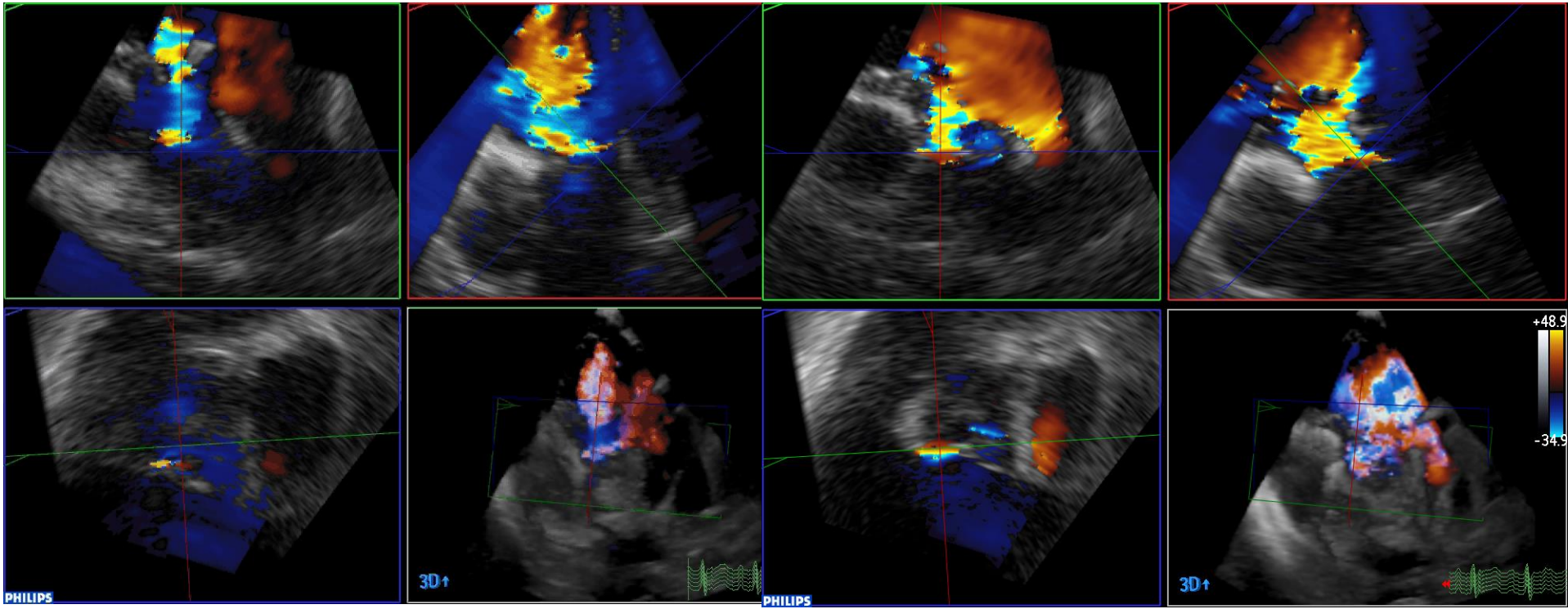

AR severity

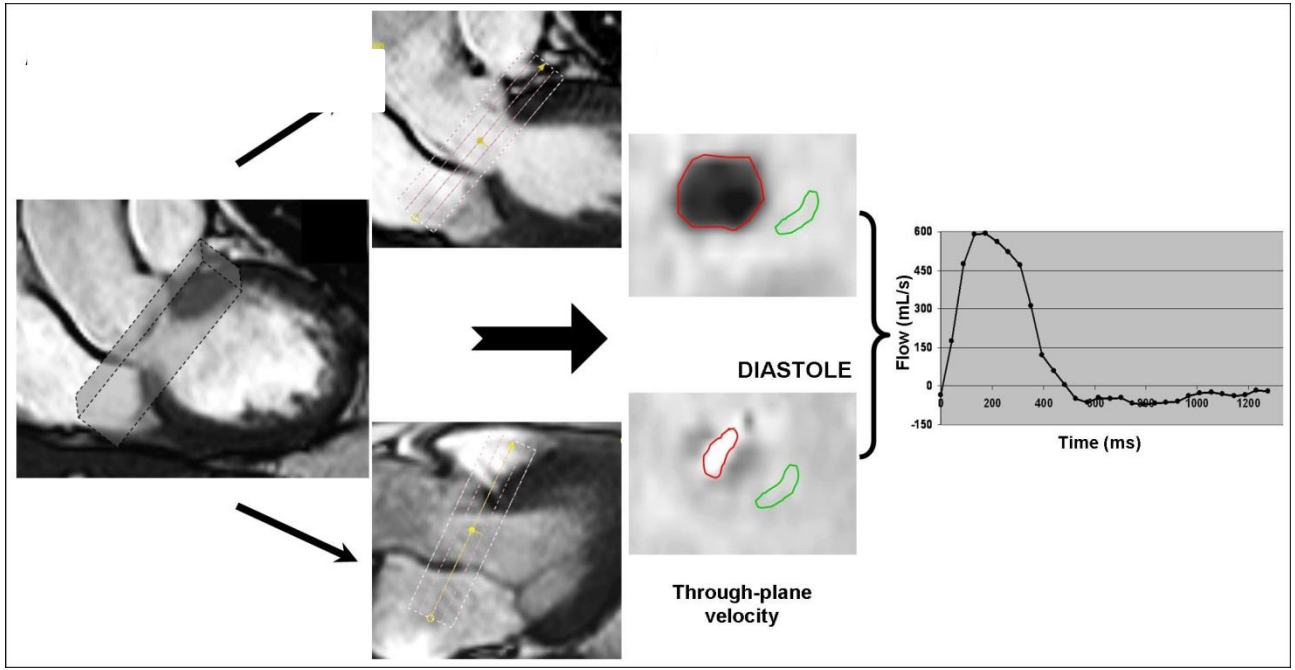

Ewe et al. Am J Cardiol 2013

AR severity

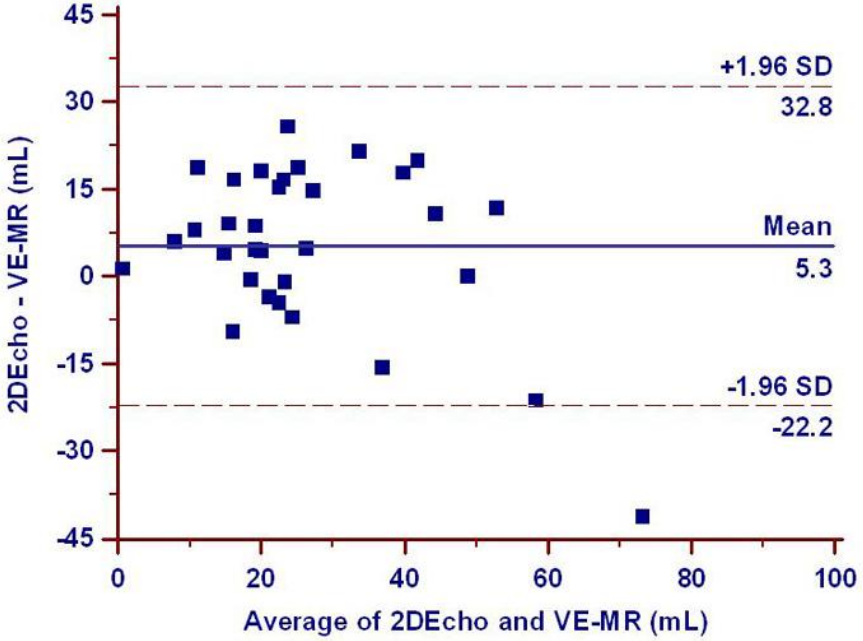

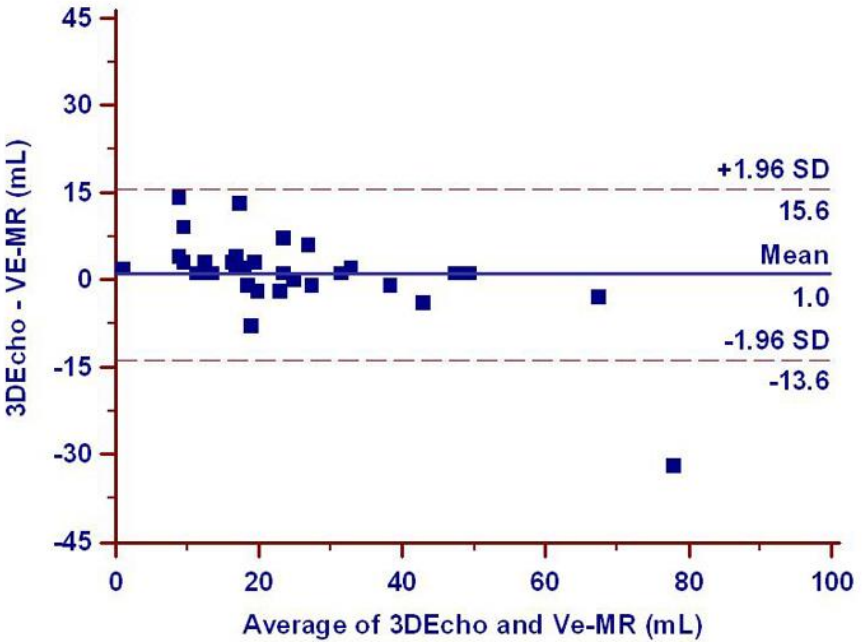

Ewe et al. Am J Cardiol 2013

AR - Mechanism

- Type 1 Enlargement of the aortic root with normal cusps
- Type 2 Cusp prolapse
- Type 3 Restrictive cusp motion

Le Polain de Waroux et al. Circ 2007

AR - Mechanism

AI Class	Type I Normal cusp motion with FAA dilatation or cusp perforation				Type II Cusp Prolapse	Type III Cusp Restriction
	Ia	Ib	Ic	Id		
Mechanism		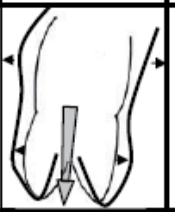	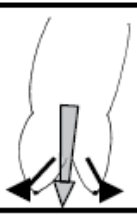			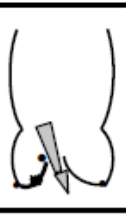
Repair Techniques (Primary)	STJ remodeling *Ascending aortic graft*	Aortic Valve sparing: *Reimplantation or Remodeling with SCA*	SCA	Patch Repair *Autologous or bovine pericardium*	Prolapse Repair *Plication* *Triangular resection* *Free margin Resuspension* *Patch*	Leaflet Repair *Shaving* *Decalcificatio* *Patch*
(Secondary)	SCA		STJ Annuloplasty	SCA	SCA	SCA

Boodhwani et al. J Thorac Cardiovasc Surg 2009

Type I AR - Mechanism

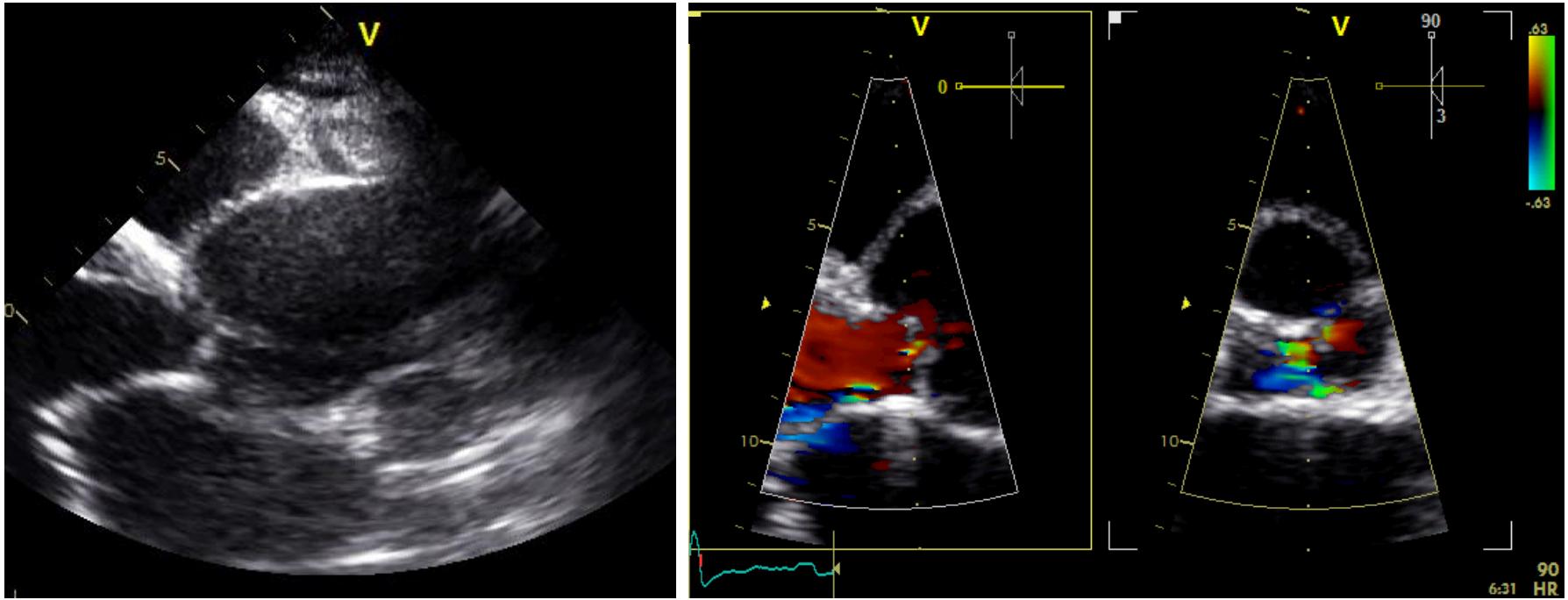

Type II AR - Mechanism

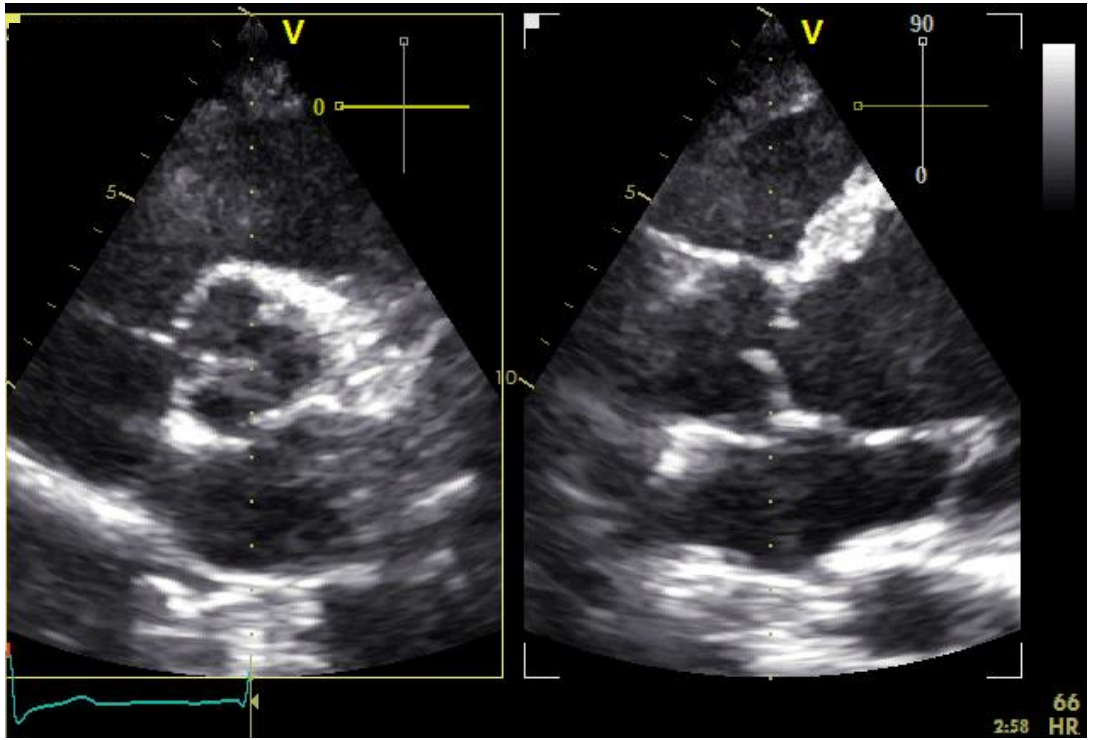

Type III AR - Mechanism

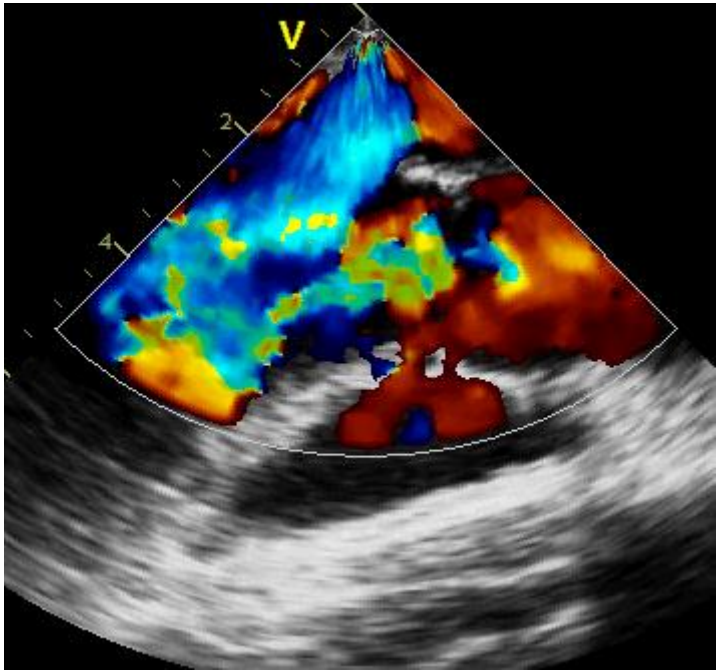

AR - Mechanism

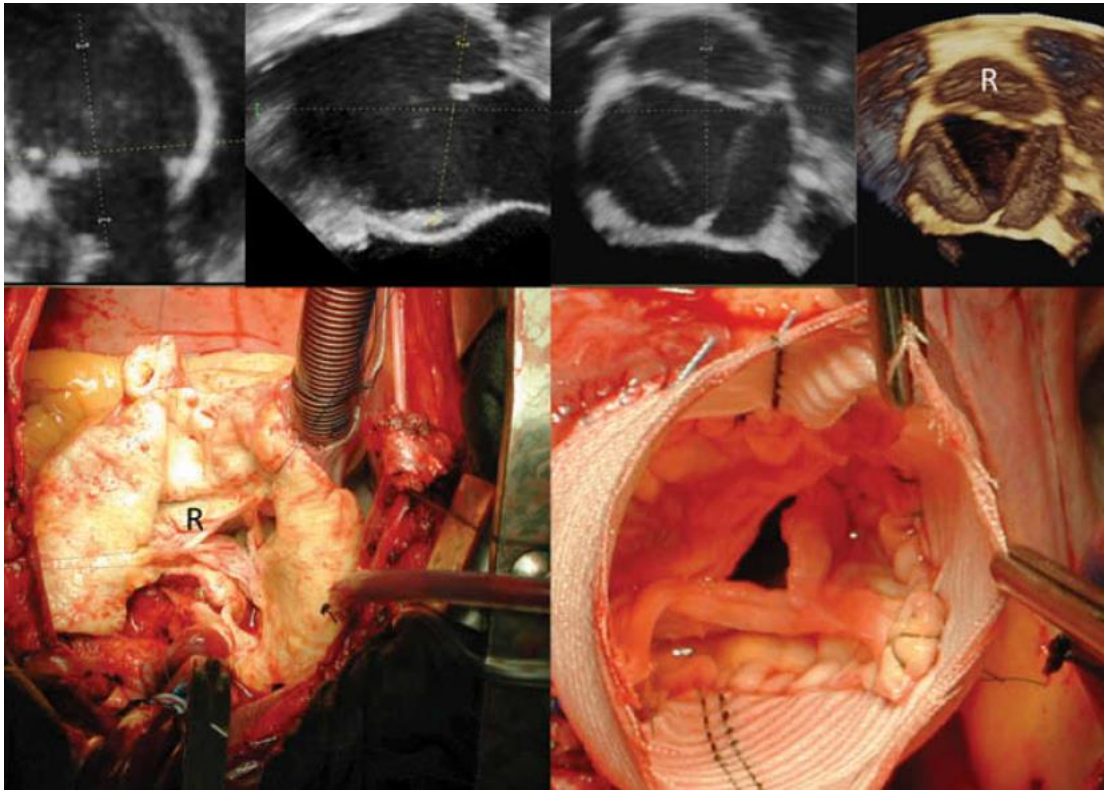

Regeer et al Expert Rev. Cardiovasc. Ther 2015

Parameters to assess repairability

CL at the central point of AV*

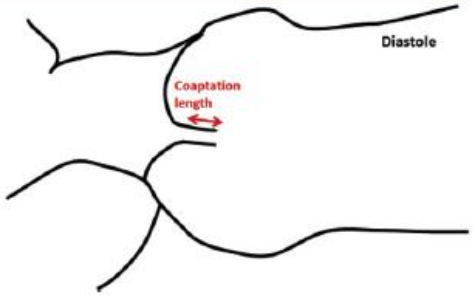

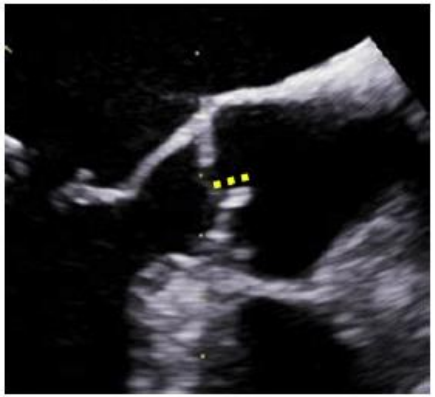

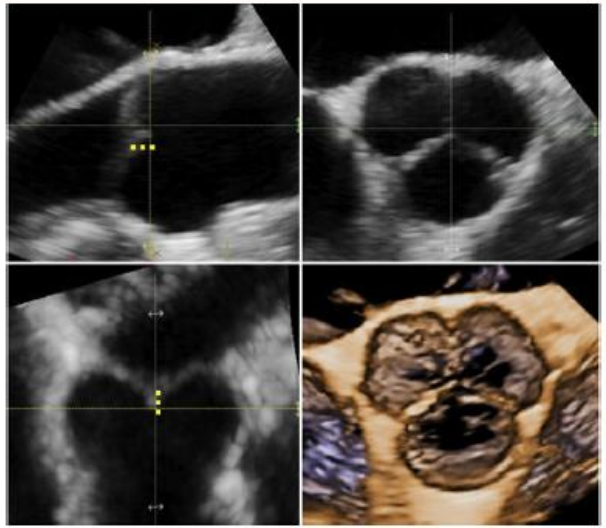

Accurate adjustment of the perpendicular sectional planes for measurement of the CL at the central point of the AV in diastole is possible only using 3D echocardiography.

Hagendorff et al J Am Coll Cardiol Img 2019;12:2225–44

Parameters to assess repairability

eH between RCC and the LCC or NCC*

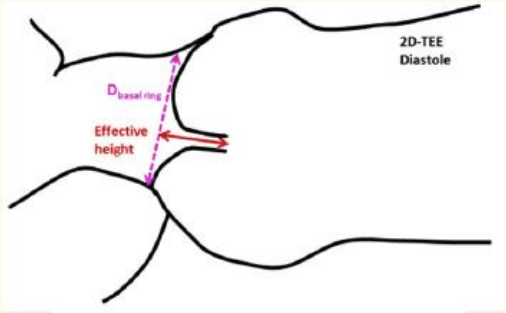

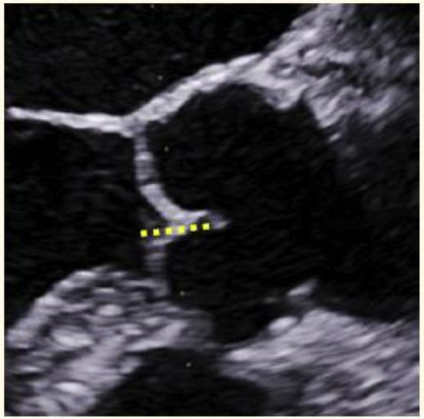

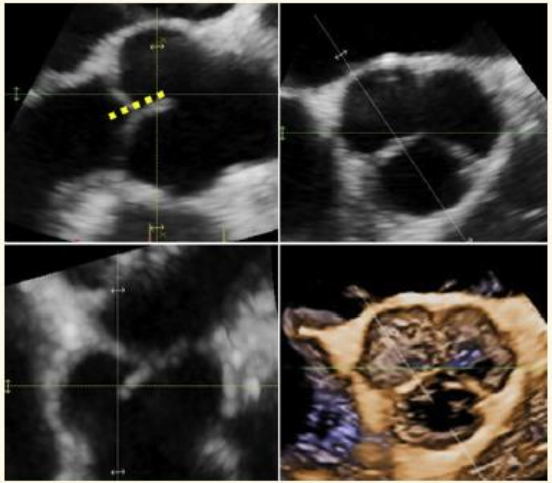

On 2D echocardiography only, the eH between the RCC and the LCC or NCC can only be determined depending on the correct orientation of the commissures. To distinguish between LCC and NCC, biplane scanning is necessary. Accurate adjustment of the perpendicular sectional planes for measurement of each eH in diastole is possible only using 3D echocardiography.

Hagendorff et al J Am Coll Cardiol Img 2019;12:2225–44

Parameters to assess repairability

Coaptation distance of the adjacent cusps*

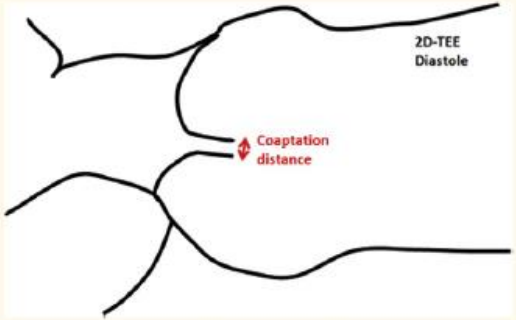

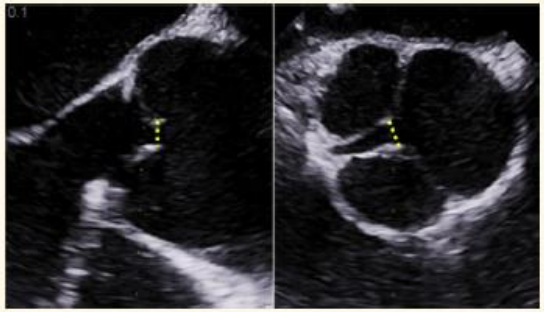

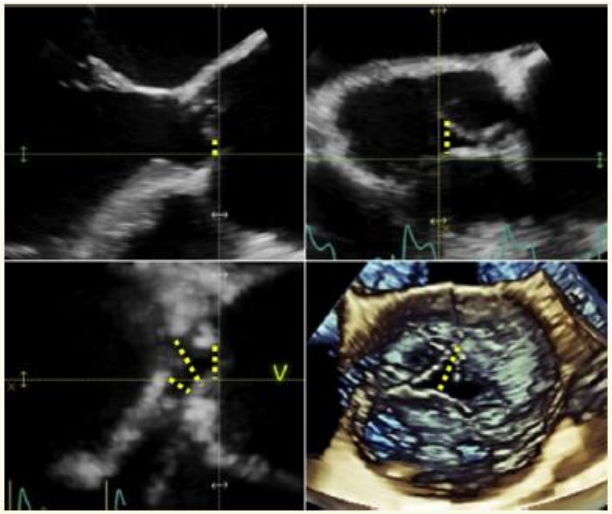

The correctness of maximum coaptation distance between the respective cusps cannot be controlled in 2D sectional planes, even if biplane scanning modalities are used. Accurate adjustment of the sectional plane perpendicular to the adjacent cusps in diastole by 3D echocardiography is necessary to assess maximum coaptation distance.

Hagendorff et al J Am Coll Cardiol Img 2019;12:2225–44

Parameters to assess repairability

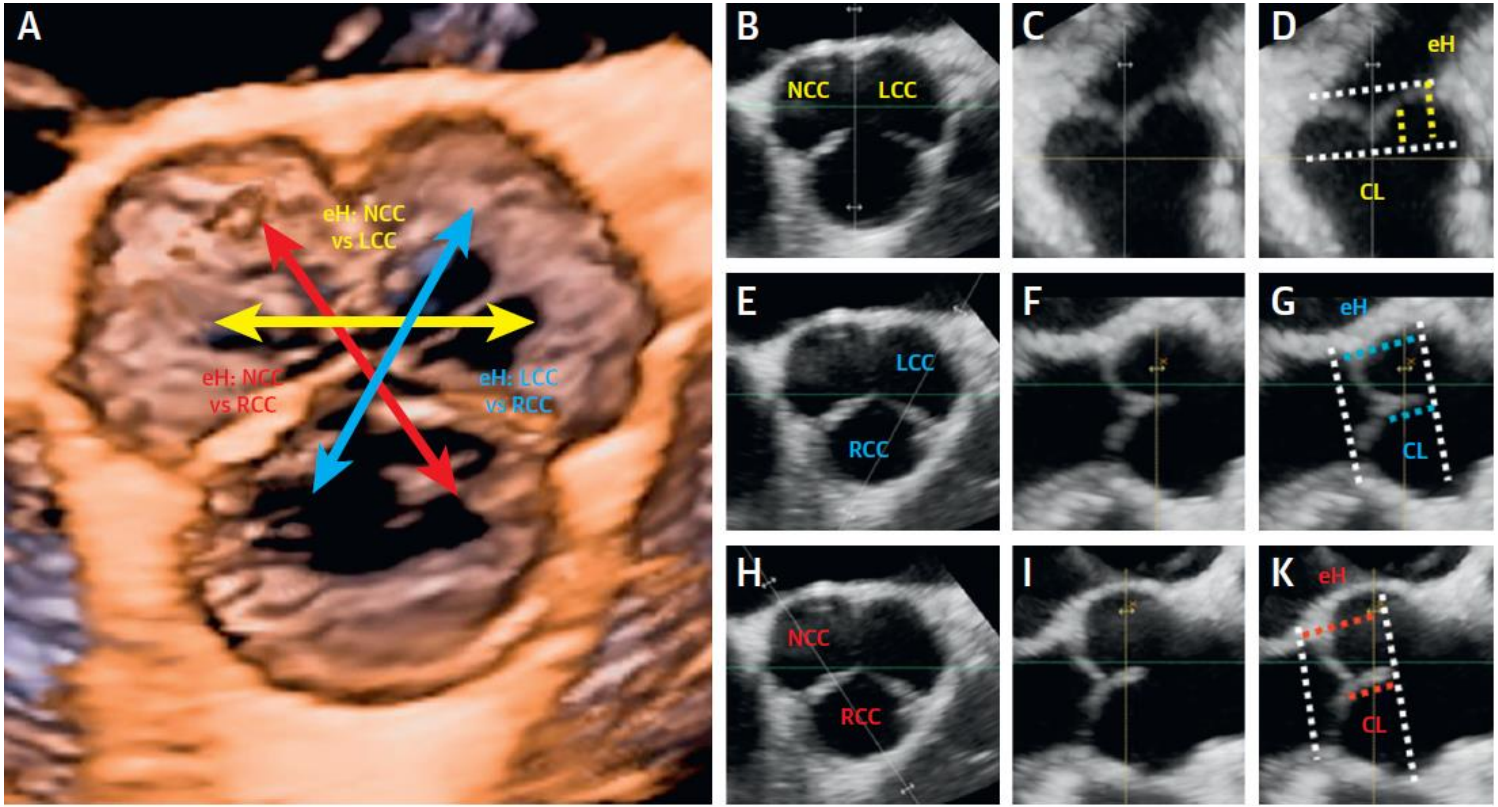

Hagendorff et al J Am Coll Cardiol Img 2019;12:2225–44

Outcome of AV repair based on type of lesion

N = 121

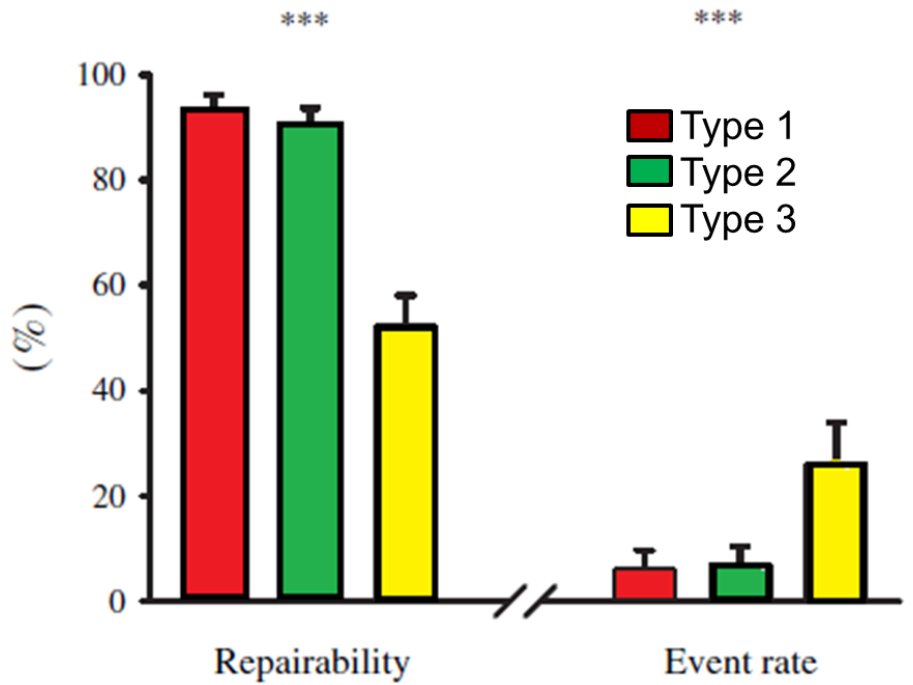

Le Polain de Waroux et al. Circ 2007

Intraoperative TEE: determinants of recurrent AR

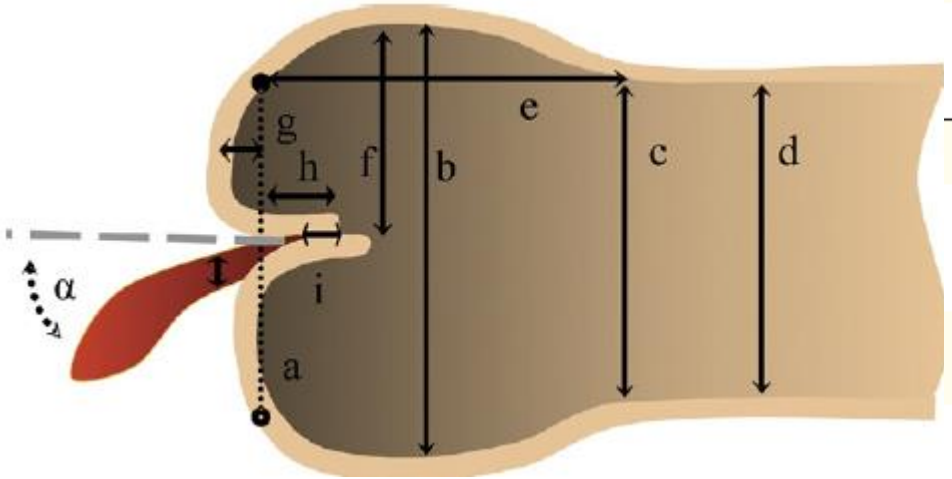

Multivariate Analysis	HR	95% Confidence Interval	Cox p Value
Coaptation length	0.82	0.63–1.00	0.05
Tips below the level of the aortic annulus	7.9	6.52–9.28	<0.01
Diameter of aortic annulus	1.18	1.03–2.45	0.01
Residual AR	5.3	1.47–6.57	0.01

Le Polain de Waroux et al. JACC Cardiovasc Imag 2009

Cusp length in TAVI for AR

LL and LD

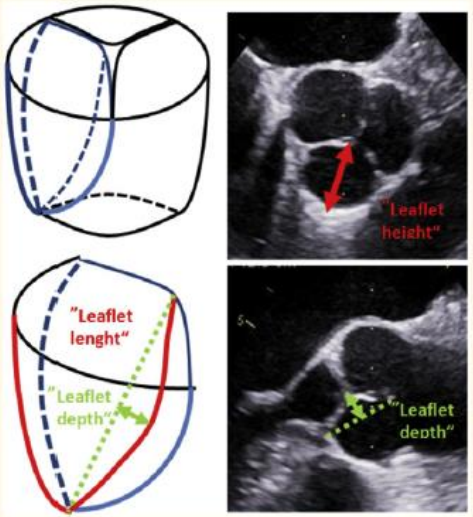

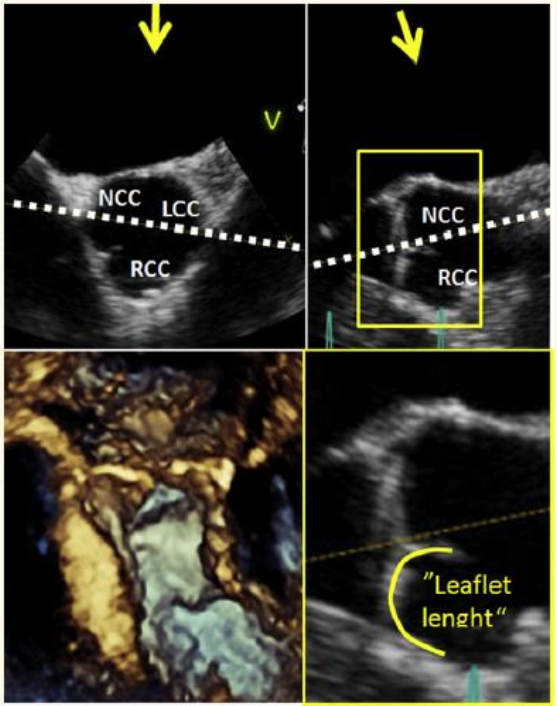

LL over the belly of the leaflet is a calculated parameter, which corresponds to the half perimeter of the ellipse described by the average LH as major axis and twice LD as minor axis. LD is measured in the long-axis view as the distance between the line from the leaflet insertion to the leaflet tip and the most convex point of the leaflet. It is possible to measure LL for each cusp using 3D echocardiography. However, LL is totally different from geometric height.

Hagendorff et al J Am Coll Cardiol Img 2019;12:2225–44

Technology Overview - JenaValve Trilogy™ Frame Design with Locator Technology

A Unique Design for Securing and Sealing Valve in Native Anatomy

- Aligns THV with Native Cusps
- Locators "Clip" onto Native Leaflets Forming a Natural Seal and Stable Securement

- Large-Open Cells Provides Access to Low Coronaries
- 24 Diamond-Shaped Cells Provide Annular Conformability and Sealing

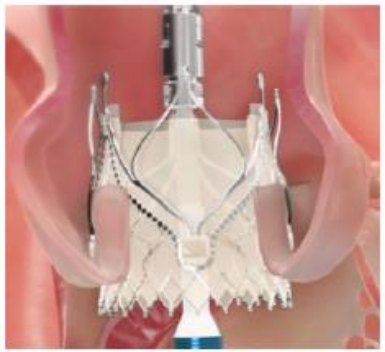

Rudolph T at EuroPCR 2022

2ND EDITION

PCR WORKSHOP

imaging
valves
madrid

Imaging for the entire HEART VALVE TEAM

Programme Directors

Pepe Zamorano - Nina Ajmone Marsan - Victoria Delgado
Madalina Garbi - Rebecca Hahn - Denisa Muraru

2-3 February 2024

Madrid, Spain

#PCRimaging

EACVI
European Association of Cardiovascular Imaging

EuroEcho-Imaging 2024

THE LEADING ECHOCARDIOGRAPHY CONGRESS

11-13 December
Berlin, Germany

#EuroEcho